Available online at www.sciencedirect.com
SCIENCE DIRECT®
Biochemical and Biophysical Research Communications 327 (2005) 100–105
BBRC
www.elsevier.com/locate/ybbrc

SOCS3/CIS3 negative regulation of STAT3 in HGF-induced keratinocyte migration

Sho Tokumaru[a], Koji Sayama[a,*], Kenshi Yamasaki[a], Yuji Shirakata[a], Yasushi Hanakawa[a], Yoko Yahata[a], Xiuju Dai[a], Mikiko Tohyama[a], Lujun Yang[a], Akihiko Yoshimura[b], Koji Hashimoto[a]

[a] *Department of Dermatology, Ehime University School of Medicine, Ehime, Japan*
[b] *Division of Molecular and Cellular Immunology, Medical Institute of Bioregulation, Kyusyu University, Fukuoka, Japan*

Received 20 November 2004
Available online 9 December 2004

Abstract

Hepatocyte growth factor (HGF) is a potent mitogen for mature hepatocytes. Because HGF has strong effects on the motility of keratinocytes and is produced by fibroblasts, HGF is thought to regulate keratinocyte migration during wound healing. However, the intracellular signaling mechanism of HGF-induced keratinocyte migration is poorly understood. In this report, we clarify the roles of STAT3 and SOCS/CIS family in HGF-induced keratinocyte migration. HGF activated STAT3 and strongly induced keratinocyte migration. Transfection with the dominant-negative mutant of STAT3 almost completely abolished HGF-induced keratinocyte migration and STAT3 phosphorylation. Next, we studied the mechanisms that regulate STAT3 phosphorylation. HGF enhanced the expression of SOCS3/CIS3 by sixfold within 1 h, but had minimum effect on SOCS1/JAB expression. Transfection with SOCS3/CIS3 almost completely abolished HGF-induced STAT3 phosphorylation and keratinocyte migration, indicating that SOCS3/CIS3 acts as a negative regulator of HGF-induced keratinocyte migration. In conclusion, SOCS3/CIS3 regulates HGF-induced keratinocyte migration by inhibiting STAT3 phosphorylation.

Keywords: Keratinocytes; HGF; Migration; STAT3; STAT1; SOCS3/CIS3; SOCS1/JAB; Wound healing; Adenovirus vector

The migration of epidermal keratinocytes is an important step in skin wound healing. Several growth factors regulate keratinocyte migration [1]. Hepatocyte growth factor (HGF) is a potent mitogen for mature hepatocytes [2,3]. HGF also has mitogenic, motogenic, morphogenic, and tumor-inhibitory activities for a variety of cells, including epithelial, endothelial, and some types of stromal cells [4–6]. Because HGF has potent effects on the motility of keratinocytes and because dermal fibroblasts produce HGF in the skin [7], HGF has been suggested to play a regulatory role in keratinocyte migration during wound healing [8,9]. Recently, an application of HGF has been demonstrated as a potential therapeutic approach for the treatment of cutaneous ulcer [10–13]. However, the intracellular signaling mechanism of HGF-induced migration is poorly understood.

c-Met is an HGF receptor that is autophosphorylated upon binding of HGF. Phosphorylated c-Met recruits a number of substrates with Src homology (SH)2 domains, such as phosphatidylinositol 3-kinase [14], Grb-2 (ASH)/Sos complex [15], Ras GTPase activating protein, $pp60^{src}$, and phospholipase C [15]. Grb-2 has also been implicated in the recruitment of the large adaptor protein Grb-2-associated binding protein-1 (Gab1) to the Met signaling complex [16–18]. These signaling molecules lead to mitogenic activity via the Ras–Raf1–MEK–MAPK pathway. In addition to these

* Corresponding author. Fax: +81 960 5352.
E-mail address: sayama@m.ehime-u.ac.jp (K. Sayama).

0006-291X/$ - see front matter © 2004 Elsevier Inc. All rights reserved.
doi:10.1016/j.bbrc.2004.11.145

pathways, two signal transducers and activators of transcription (STAT) proteins, STAT1 and STAT3, are signaling cascade proteins located downstream from c-Met [19].

The STAT signaling pathways are negatively regulated by proteins of the suppressor of cytokine signaling (SOCS)/cytokine-inducible SH2-containing protein (CIS) family to avoid oversignaling [20]. The SOCS/CIS family is induced by cytokine stimulation and binds to tyrosine-phosphorylated sites of the cytokine receptor or to Jak through an SH2 domain, resulting in the inhibition of tyrosine kinase phosphorylation. CIS was the first member of the SOCS/CIS family to be identified; it binds to the tyrosine-phosphorylated site of the erythropoietin receptor and inhibits the STAT5 signal downstream [21]. Additional members of the SOCS/CIS family have been identified independently [22,23]. SOCS1/JAB binds mainly to Jak2 [24] and regulates the IFN-γ/STAT1 [25] and IL-6/STAT3 signaling pathways [23]. SOCS2/CIS2 regulates insulin-like growth factor and the insulin-like growth factor receptor signaling pathways [26]. SOCS3/CIS3 regulates the IL-6/STAT3 and IFN-γ/STAT1 signaling pathways.

Because STATs are involved in the HGF-c-Met signaling pathway, we hypothesized that the SOCS/CIS family regulates HGF-induced keratinocyte migration by inhibiting STAT pathways. To prove this, we first studied whether STAT3 was involved in HGF-induced keratinocyte migration. Next, we tested whether the SOCS/CIS family affects HGF-induced keratinocyte migration through the inhibition of STAT3.

Materials and methods

Reagents and antibodies. Recombinant HGF was kindly provided by Dr. Kunio Matsumoto (Osaka University, Osaka, Japan). Antibodies were purchased as follows: mouse monoclonal STAT3 (Transduction Laboratories) and phospho-STAT3 (New England Biolabs).

Keratinocyte culture. Human skin samples were obtained after plastic surgery under a protocol approved by the Institutional Review Board of Ehime University School of Medicine. Primary normal human keratinocytes were isolated from the normal human skin. Normal human keratinocytes were cultured with MCDB153 medium supplemented with insulin (1 μg/ml), hydrocortisone (0.5 μM), ethanolamine (0.1 mM), phosphoethanolamine (0.1 mM), bovine hypothalamic extract (BHE; 50 μg/ml), and Ca^{2+}(0.1 mM). This supplement was as described elsewhere [27].

Migration assay. Keratinocytes were cultured at 1×10^5 cells per 35-mm type I-collagen-coated culture plate in culture medium without BHE for 12 h. After stimulation, keratinocyte migration was observed using time-lapse video microscopy (IX-IBC, CK30; Olympus, Tokyo, Japan) in a controlled chamber at 37 °C and 5% CO_2.

Keratinocyte migration was assayed quantitatively with a Boyden chamber, as previously described [28]. Designated amounts of HGF were added to the bottom wells of a 48-well Boyden chamber (Neuro Probe, Cabin John, MD), and an 8-μm pore-size polyvinylpyrrolidone-free polycarbonate membrane (Neuro Probe) was placed on the wells. The membrane was precoated with type I collagen (10 μg/ml in PBS, Nitta Gelatin, Osaka, Japan) at room temperature for 1 h and then extensively washed with PBS. Subconfluent keratinocytes were harvested with trypsin–EDTA (0.05% trypsin and 0.5 mM EDTA) and resuspended in the culture medium without BHE at 1×10^5 cells/ml. Fifty microliters of the keratinocyte suspension (5000 cells/well) was added to the upper wells, and the chamber was incubated overnight at 37 °C in a humidified atmosphere of air with 5% CO_2. Cells that adhered to the upper surface of the filter membrane were removed by scraping with a rubber blade. Cells that moved through the filter and stayed on the lower surface of the membrane were considered to be migrated cells. The membrane was fixed with 10% buffered formalin overnight and then stained with Gill's hematoxylin overnight. The membrane was then mounted between two glass slides with 90% glycerol and the number of migrated cells was determined by counting under a microscope.

Western blotting. Subconfluent keratinocytes were starved for 2 h in BHE-free medium and stimulated with HGF as indicated. Cells were harvested on ice in lysis buffer containing 5 mM EDTA, 100 μM sodium orthovanadate, 100 μM sodium pyrophosphate, 1 mM sodium fluoride, 5 μM 3,4-dichloroisocoumarin, 1 μg/ml aprotinin, and 1% Triton X-100 in PBS. Twenty micrograms of protein was separated on 10% SDS–PAGE and then transferred to a PVDF membrane. The membranes were blocked with 5% skimmed milk in PBS overnight at 4 °C. The blocked membranes were incubated for 6 h with the first antibody as indicated. After three washes with PBS containing 0.05% Tween 20, the membranes were treated with ABC reagents (VECTOR Laboratories, Burlingame, CA) for 20 min at room temperature, washed three times with PBS containing 0.05% Tween 20, treated with ECL detection reagents (Amersham–Pharmacia Biotech, Piscataway, NJ) for 1 min at room temperature, and then exposed to films (Kodak, Rochester, NY).

Quantitative PCR analysis. Total RNA from cultured human keratinocytes was prepared using Isogen (Nippon Gene, Toyama, Japan) and was treated with 50 U/ml DNase I (Clontech) at 37 °C for 30 min to remove any genomic DNA contamination.

To quantify the mRNA expression in vivo, we performed quantitative RT-PCR using the ABI Prism 7700 sequencer detection system (Perkin–Elmer Applied Biosystems, Foster City, CA). RT-PCR mixtures were prepared according to the manufacturer's instructions for the TaqMan One-Step RT-PCR Master Mix Reagent kit (Perkin–Elmer Applied Biosystems). Briefly, 50 ng of total RNA was added to each 50-μl reaction mixture containing 1 μl master mix, 1× multiScribe and RNase inhibitor mix, 200 nM of each primer, and 100 nM hybridization probe for specific detection of target cDNA. For SOCS1/JAB detection, the sense primer 5′-TTTTTCGCCCTTAGC GTGAA-3′, the antisense primer 5′-GCCATCCAGGTGAAAGCG-3′, and the probe 5′-CCTCGGGACCCACGAGCATCC-3′ were added. For SOCS3/CIS3 detection, the sense primer 5′-TTCAGCA TCTCTGTCGGAAGAC-3′, the antisense primer 5′-GCATCGTAC TGGTCCAGGAACT-3′, and the probe 5′-AACGGCCACCTGG ACTCCTATGAGAAA-3′ were added. The probe was labeled with a reporter fluorescent dye, FAM (6-carboxyfluorescein), at the 5′-end. For GAPDH detection, 1 μl of Pre-Developed TaqMan Assay Reagent (Perkin–Elmer Applied Biosystems) was added. The thermal conditions were 48 °C for 30 min for reverse transcription and 95 °C for 10 min, followed by 45 amplification cycles of 95 °C for 15 s for denaturing and 55 °C for 1.5 min for annealing and extension. The PCR products were sequenced to confirm the proper amplification. To compare mRNA expression, the results were estimated as relative values using GAPDH as an internal reference. The relative quantified expression was calculated using the following formula: relative expression $= 2[-(\sum CT_s/N_s - \sum CT_{GAPDH_s}/N_s) - (\sum CT_r/N_r - \sum CT_{GAPDH_r}/N_r)]$, where CT_s denotes the cycle threshold for the candidate gene in the sample, N_s is the number of samples, CT_{GAPDH_s} is the cycle threshold for GAPDH in the same sample, CT_r is the cycle threshold for the candidate gene in the overall reference sample, N_r is the number of reference samples, and CT_{GAPDH_r} is the cycle threshold for GAPDH in the same reference sample. In each group, there were $n = 3$ samples.

Adenovirus vectors (Ax). STAT3 has a phosphorylation site at tyrosine705. In the dominant negative mutants of STAT3 (STAT3F), the phosphorylatable tyrosine residue is substituted with phenylalanine. Axs encoding STAT3F (AxCA STAT3F), SOCS1/JAB (AxCAJAB), and SOCS3/CIS3 (AxCACIS3) were generated as previously described [29] using the COS–TPC method [30]. Ax encoding lacZ (Ax LacZ) was a gift from Dr. Izumi Saito (University of Tokyo). Virus stocks were prepared using a standard procedure [30]. Concentrated, purified virus stocks were prepared using a CsCl gradient, and the virus titer was checked using a plaque formation assay. We infected normal human keratinocytes with Ax at a multiplicity of infection (MOI) of five.

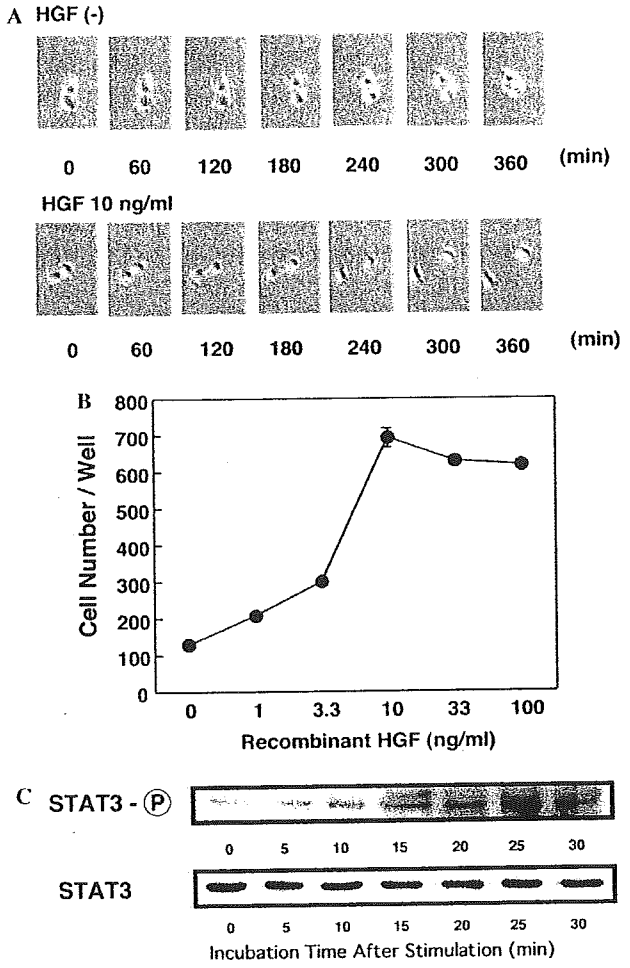

Fig. 1. Keratinocyte migration and phosphorylation of STAT3 by HGF. (A) HGF-induced keratinocyte migration. After adding 10 ng/ml HGF, keratinocyte migration was observed under time-lapse video microscopy every 60 min. (B) Quantification of keratinocyte migration induced by HGF. The indicated amount of HGF was added to the bottom wells of a 48-well Boyden chamber, and then an 8-μm pore-size polyvinylpyrrolidone-free polycarbonate membrane was placed on the wells. Keratinocytes were added to the upper wells at 5000 cells/well. After overnight incubation, the membrane was stained with Gill's hematoxylin. The number of cells that had migrated through the filter was determined by counting under a microscope. Each point shows means ± SD of quadruplicate measurements. (C) Phosphorylation of STAT3 by HGF. Subconfluent keratinocytes were starved for 2 h in BHE-free medium and stimulated with 10 ng/ml HGF. Cells were harvested and the phosphorylation of STAT3 was analyzed by Western blotting.

Results

HGF induces keratinocyte migration and phosphorylates STAT3

We first observed whether HGF induces the migration of normal human keratinocytes by using time-lapse video microscopy (Fig. 1A). Keratinocytes started to migrate within 180 min after HGF stimulation. Without HGF, no migration occurred. Then, the migration was analyzed quantitatively using the Boyden chamber assay (Fig. 1B). HGF induced keratinocyte migration sixfold that of control. The optimum concentration of HGF was 10 ng/ml. The phosphorylation of STAT3 was analyzed by Western blotting (Fig. 1C). HGF phosphorylated STAT3 at 25 min.

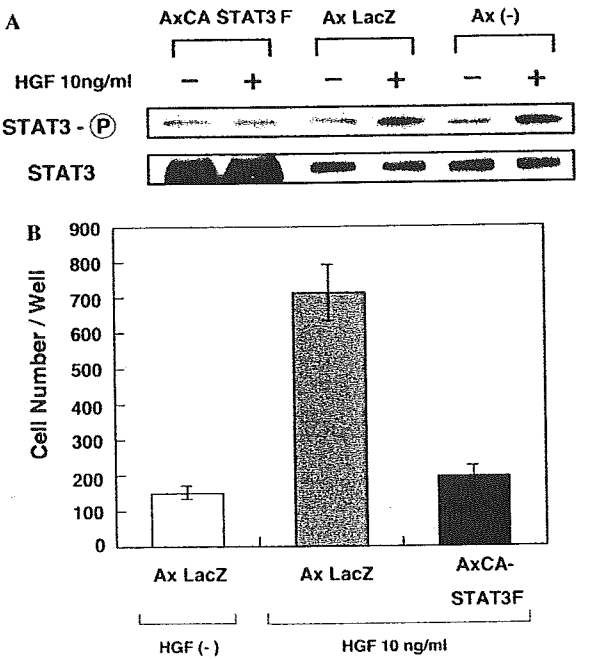

Fig. 2. Inhibition of HGF-induced phosphorylation of STAT3 and keratinocyte migration by STAT3F. (A) Inhibition of STAT3 phosphorylation. Ax LacZ and AxCA STAT3F were transfected into normal human keratinocytes at an MOI of 5. After 24 h, the keratinocytes were stimulated with 10 ng/ml HGF or vehicle alone for 25 min. Then the cells were harvested and analyzed by Western blotting. (B) Inhibition of keratinocyte migration. Ax LacZ and AxCA STAT3F were transfected into normal human keratinocytes at an MOI of five. After 24 h, the keratinocytes were harvested and transferred to a Boyden chamber and HGF (10 ng/ml) was added to the lower chamber. The migration was analyzed as in Fig. 1B. Each point shows the mean ± SD of quadruplicate measurements.

Phosphorylation of STAT3 is essential for HGF-induced keratinocyte migration

We next constructed dominant negative mutants of STAT3 (STAT3F) to study the role of STAT3 in HGF-induced keratinocyte migration. The expression of STAT3F using Ax (AxCA STAT3F) almost completely blocked HGF-induced STAT3 phosphorylation, while the transfection of LacZ had no effect on the STAT3 phosphorylation (Fig. 2A).

Using AxCA STAT3F, we analyzed the functions of STAT3 in HGF-induced keratinocyte migration. After the transfection of keratinocytes with AxCA STAT3F, the HGF-induced migration of the keratinocytes was quantitatively analyzed with the Boyden chamber assay (Fig. 2B). The expression of STAT3F almost completely blocked HGF-induced keratinocyte migration, while the expression of LacZ had no effect on migration. Because STAT3 was phosphorylated by HGF, and because HGF-induced migration was blocked by STAT3F, we concluded that the phosphorylation of STAT3 is essential for HGF-induced keratinocyte migration.

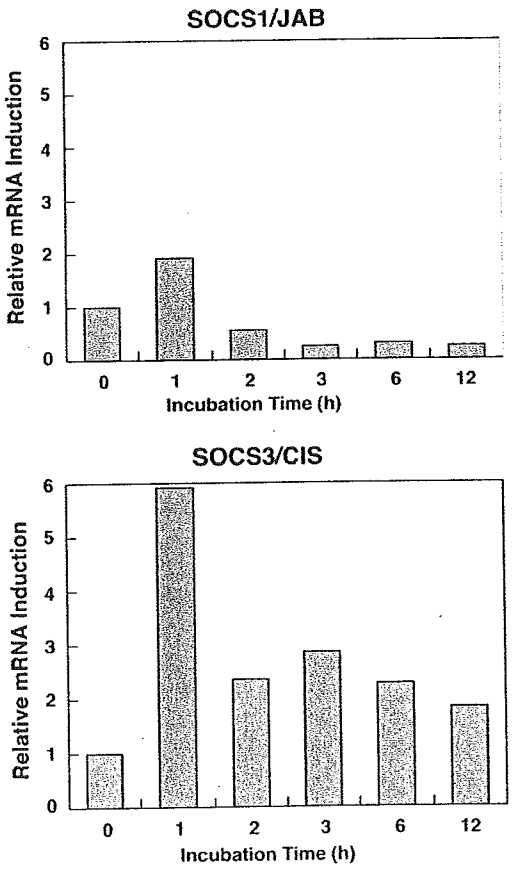

Fig. 3. Induction of SOCS3/CIS by HGF. Subconfluent keratinocytes were stimulated with 10 ng/ml HGF. Cells were harvested at the indicated time. The mRNA expression of SOCS1/JAB and SOCS3/CIS was analyzed using real-time PCR. The results were adjusted to relative values using GAPDH as an internal reference.

HGF induces SOCS3/CIS3

The SOCS/CIS family is inducible de novo by stimulation and negatively regulates the STAT family. Therefore, it is possible that the SOCS/CIS family regulates HGF-induced keratinocyte migration. To prove this, we first determined whether HGF induces the SOCS/CIS family in keratinocytes. As shown in Fig. 3, HGF enhanced the SOCS3/CIS3 mRNA expression sixfold at 1 h after stimulation, while the induction of SOCS1/JAB by HGF was not as significant as that of SOCS3/CIS3.

SOCS1/JAB and SOCS3/CIS3 inhibit HGF-induced STAT3 phosphorylation and keratinocyte migration

First, we determined the effects of SOCS1/JAB and SOCS3/CIS3 on HGF-induced STAT3 phosphorylation. AxCAJAB and AxCACIS3 were transfected into keratinocytes; the expression of either SOCS1/JAB or SOCS3 / CIS3 almost completely blocked HGF-induced STAT3 phosphorylation (Fig. 4A).

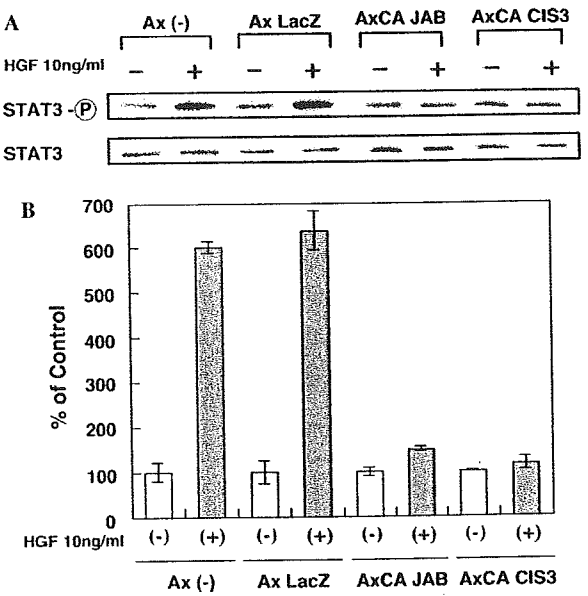

Fig. 4. Inhibition of HGF-induced STAT3 phosphorylation and keratinocyte migration by SOCS1/JAB and SOCS3/CIS3. (A) Inhibition of STAT3 phosphorylation. Ax LacZ, AxCAJAB, and AxCACIS3 were transfected into normal human keratinocytes at an MOI of 5. After 24 h, the keratinocytes were stimulated with 10 ng/ml HGF or vehicle alone for 25 min. Then, the cells were harvested and analyzed by Western blotting. (B) Inhibition of keratinocyte migration. Ax LacZ, AxCAJAB, and AxCACIS3 were transfected into normal human keratinocytes at an MOI of 5. After 24 h, the keratinocytes were harvested and transferred to a Boyden chamber for the analysis of migration, as described in Fig. 1B. HGF (10 ng/ml) was added to the lower chamber, and the set-up was incubated overnight. Each point shows the mean ± SD of quadruplicate measurements.

Using AxCAJAB and AxCACIS3, we analyzed the regulatory mechanism of STAT3 in HGF-induced keratinocyte migration. After the transfection of keratinocytes with AxCAJAB or AxCACIS3, the HGF-induced migration of the keratinocytes was analyzed quantitatively with the Boyden chamber assay (Fig. 4B). The expression of either SOCS1/JAB or SOCS3/CIS3 almost completely blocked HGF-induced keratinocyte migration. Because SOCS3/CIS3 was induced by HGF and SOCS3/CIS3 blocked HGF-induced phosphorylation of STAT3 and migration, we concluded that SOCS3/CIS3 regulates HGF-induced keratinocyte migration.

Discussion

The intracellular signaling mechanisms involving c-Met have been studied in hepatocytes primarily. Although it was demonstrated that HGF induces keratinocyte migration [8], the intracellular signaling mechanisms remained unclear. It was suggested that the major signaling pathway downstream from HGF/c-Met is the MAPK cascade [31]. However, the involvement of STAT signaling cascades in HGF-induced signal transduction was also reported [19]. Because EGF-induced keratinocyte migration was abolished in STAT3-disrupted keratinocytes [32], STAT pathways were thought to be involved in HGF-induced keratinocyte migration. Therefore, we studied whether SOCS/CIS regulates HGF-induced keratinocyte migration.

The SOCS/CIS family negatively regulates STAT pathways. However, the inhibitory functions of the SOCS/CIS family differ among cell types and cell conditions. In this study, we showed that SOCS3/CIS3 was induced and inhibited STAT3 phosphorylation and migration, indicating that SOCS3/CIS3 acts as a self-limiting factor to avoid overstimulation. Although HGF induces SOCS3/CIS3, EGF, a growth factor that strongly induces keratinocyte migration [33], does not induce SOCS1/JAB or SOCS3/CIS3 [29]. Therefore, EGF-induced keratinocyte migration does not involve the SOCS1/JAB- or SOCS3/CIS3-mediated self-regulatory mechanism of STAT3 activation in keratinocytes. This indicates that the intracellular regulatory mechanism of keratinocyte migration differs among growth factors.

In this study, we showed that SOCS1/JAB inhibited HGF-induced keratinocyte migration. However, SOCS1/JAB was not induced by HGF, suggesting that SOCS1/JAB has another role other than acting as a self-limiting factor. It is possible that cytokine-induced SOCS1/JAB or SOCS3/CIS3 affects HGF-induced keratinocyte migration. Although the inhibitory and negative regulatory mechanisms of cytokine signals in epidermal keratinocytes have not been assessed fully, cytokines such as IFN-γ, IL-4, and IL-6 are implicated in a variety of physiological and pathological conditions of the skin. IFN-γ enhances SOCS1/JAB and SOCS3/CIS3 expression [29]. In addition, IL-4 and IL-6 enhance the expression of SOCS1/JAB and SOCS3/CIS3, respectively [29]. Therefore, cytokines in various inflammatory skin conditions might affect wound healing by regulating keratinocyte migration via the induction of SOCS1/JAB or SOCS3/CIS3.

In conclusion, the SOCS3/CIS3 negative feedback mechanism of STAT3 activation is a key pathway of HGF-induced keratinocyte migration.

Acknowledgments

We thank Teruko Tsuda and Eriko Tan for their excellent technical assistance.

References

[1] Y. Sarret, D.T. Woodley, K. Grigsby, K. Wynn, E.J. O'Keefe, Human keratinocyte locomotion: the effect of selected cytokines, J. Invest. Dermatol. 98 (1992) 12–16.
[2] T. Nakamura, K. Nawa, A. Ichihara, Partial purification and characterization of hepatocyte growth factor from serum of hepatectomized rats, Biochem. Biophys. Res. Commun. 122 (1984) 1450–1459.
[3] W.E. Russell, J.A. McGowan, N.L. Bucher, Biological properties of a hepatocyte growth factor from rat platelets, J. Cell. Physiol. 119 (1984) 193–197.
[4] K. Matsumoto, T. Nakamura, Hepatocyte growth factor (HGF) as a tissue organizer for organogenesis and regeneration, Biochem. Biophys. Res. Commun. 239 (1997) 639–644.
[5] C. Birchmeier, E. Gherardi, Developmental roles of HGF/SF and its receptor, the c-Met tyrosine kinase, Trends Cell Biol. 8 (1998) 404–410.
[6] Y.W. Zhang, G.F. Vande Woude, HGF/SF-met signaling in the control of branching morphogenesis and invasion, J. Cell. Biochem. 88 (2003) 408–417.
[7] E. Gohda, H. Kataoka, H. Tsubouchi, Y. Daikilara, I. Yamamoto, Phorbol ester-induced secretion of human hepatocyte growth factor by human skin fibroblasts and its inhibition by dexamethasone, FEBS Lett. 301 (1992) 107–110.
[8] K. Matsumoto, K. Hashimoto, K. Yoshikawa, T. Nakamura, Marked stimulation of growth and motility of human keratinocytes by hepatocyte growth factor, Exp. Cell Res. 196 (1991) 114–120.
[9] R. Tsuboi, C. Sato, C.M. Shi, H. Ogawa, Stimulation of keratinocyte migration by growth factors, J. Dermatol. 19 (1992) 652–653.
[10] S. Yoshida, K. Matsumoto, D. Tomioka, K. Bessho, S. Itami, K. Yoshikawa, T. Nakamura, Recombinant hepatocyte growth factor accelerates cutaneous wound healing in a diabetic mouse model, Growth Factors 22 (2004) 111–119.
[11] K. Nakanishi, M. Uenoyama, N. Tomita, R. Morishita, Y. Kaneda, T. Ogihara, K. Matsumoto, T. Nakamura, A. Maruta, S. Matsuyama, T. Kawai, T. Aurues, T. Hayashi, T. Ikeda, Gene transfer of human hepatocyte growth factor into rat skin wounds mediated by liposomes coated with the Sendai virus (hemagglutinating virus of Japan), Am. J. Pathol. 161 (2002) 1761–1772.

[12] D. Bevan, E. Gherardi, T.P. Fan, D. Edwards, R. Warn, Diverse and potent activities of HGF/SF in skin wound repair, J. Pathol. 203 (2004) 831–838.
[13] I. Ono, T. Yamashita, T. Hida, H.Y. Jin, Y. Ito, H. Hamada, Y. Akasaka, T. Ishii, K. Jimbow, Local administration of hepatocyte growth factor gene enhances the regeneration of dermis in acute incisional wounds, J. Surg. Res. 120 (2004) 47–55.
[14] A. Graziani, D. Gramaglia, L.C. Cantley, P.M. Comoglio, The tyrosine-phosphorylated hepatocyte growth factor/scatter factor receptor associates with phosphatidylinositol 3-kinase, J. Biol. Chem. 266 (1991) 22087–22090.
[15] C. Ponzetto, A. Bardelli, Z. Zhen, F. Maina, P. dalla Zonca, S. Giordano, A. Graziani, G. Panayotou, P.M. Comoglio, A multifunctional docking site mediates signaling and transformation by the hepatocyte growth factor/scatter factor receptor family, Cell 77 (1994) 261–271.
[16] A. Bardelli, P. Longati, D. Gramaglia, M.C. Stella, P.M. Comoglio, Gab1 coupling to the HGF/Met receptor multifunctional docking site requires binding of Grb2 and correlates with the transforming potential, Oncogene 15 (1997) 3103–3111.
[17] L. Nguyen, M. Holgado-Madruga, C. Maroun, E.D. Fixman, D. Kamikura, T. Fournier, A. Charest, M.L. Tremblay, A.J. Wong, M. Park, Association of the multisubstrate docking protein Gab1 with the hepatocyte growth factor receptor requires a functional Grb2 binding site involving tyrosine 1356, J. Biol. Chem. 272 (1997) 20811–20819.
[18] C.R. Maroun, M. Holgado-Madruga, I. Royal, M.A. Naujokas, T.M. Fournier, A.J. Wong, M. Park, The Gab1 PH domain is required for localization of Gab1 at sites of cell-cell contact and epithelial morphogenesis downstream from the met receptor tyrosine kinase, Mol. Cell. Biol. 19 (1999) 1784–1799.
[19] C. Boccaccio, M. Ando, L. Tamagnone, A. Bardelli, P. Michieli, C. Battistini, P.M. Comoglio, Induction of epithelial tubules by growth factor HGF depends on the STAT pathway, Nature 391 (1998) 285–288.
[20] R.J. Duhe, L.H. Wang, W.L. Farrar, Negative regulation of Janus kinases, Cell Biochem. Biophys. 34 (2001) 17–59.
[21] A. Yoshimura, T. Ohkubo, T. Kiguchi, N.A. Jenkins, D.J. Gilbert, N.G. Copeland, T. Hara, A. Miyajima, A novel cytokine-inducible gene CIS encodes an SH2-containing protein that binds to tyrosine-phosphorylated interleukin 3 and erythropoietin receptors, EMBO J. 14 (1995) 2816–2826.
[22] T.A. Endo, M. Masuhara, M. Yokouchi, R. Suzuki, H. Sakamoto, K. Mitsui, A. Matsumoto, S. Tanimura, M. Ohtsubo, H. Misawa, T. Miyazaki, N. Leonor, T. Taniguchi, T. Fujita, Y. Kanakura, S. Komiya, A. Yoshimura, A new protein containing an SH2 domain that inhibits JAK kinases, Nature 387 (1997) 921–924.
[23] T. Naka, M. Narazaki, M. Hirata, T. Matsumoto, S. Minamoto, A. Aono, N. Nishimoto, T. Kajita, T. Taga, K. Yoshizaki, S. Akira, T. Kishimoto, Structure and function of a new STAT-induced STAT inhibitor, Nature 387 (1997) 924–929.
[24] H. Yasukawa, H. Misawa, H. Sakamoto, M. Masuhara, A. Sasaki, T. Wakioka, S. Ohtsuka, T. Imaizumi, T. Matsuda, J.N. Ihle, A. Yoshimura, The JAK-binding protein JAB inhibits Janus tyrosine kinase activity through binding in the activation loop, EMBO J. 18 (1999) 1309–1320.
[25] W.S. Alexander, R. Starr, J.E. Fenner, C.L. Scott, E. Handman, N.S. Sprigg, J.E. Corbin, A.L. Cornish, R. Darwiche, C.M. Owczarek, T.W. Kay, N.A. Nicola, P.J. Hertzog, D. Metcalf, D.J. Hilton, SOCS1 is a critical inhibitor of interferon gamma signaling and prevents the potentially fatal neonatal actions of this cytokine, Cell 98 (1999) 597–608.
[26] D. Metcalf, C.J. Greenhalgh, E. Viney, T.A. Willson, R. Starr, N.A. Nicola, D.J. Hilton, W.S. Alexander, Gigantism in mice lacking suppressor of cytokine signalling-2, Nature 405 (2000) 1069–1073.
[27] K. Midorikawa, K. Sayama, Y. Shirakata, Y. Hanakawa, L. Sun, K. Hashimoto, Expression of vitamin D receptor in cultured human keratinocytes and fibroblasts is not altered by corticosteroids, J. Dermatol. Sci. 21 (1999) 8–12.
[28] S. Boyden, The chemotactic effect of mixtures of antibody and antigen on polymorphonuclear leucocytes, J. Exp. Med. 115 (1962) 453–466.
[29] K. Yamasaki, Y. Hanakawa, S. Tokumaru, Y. Shirakata, K. Sayama, T. Hanada, A. Yoshimura, K. Hashimoto, Suppressor of cytokine signaling 1/JAB and suppressor of cytokine signaling 3/cytokine-inducible SH2 containing protein 3 negatively regulate the signal transducers and activators of transcription signaling pathway in normal human epidermal keratinocytes, J. Invest. Dermatol. 120 (2003) 571–580.
[30] S. Miyake, M. Makimura, Y. Kanegae, S. Harada, Y. Sato, K. Takamori, C. Tokuda, I. Saito, Efficient generation of recombinant adenoviruses using adenovirus DNA-terminal protein complex and a cosmid bearing the full-length virus genome, Proc. Natl. Acad. Sci. USA 93 (1996) 1320–1324.
[31] D. Tulasne, R. Paumelle, K.M. Weidner, B. Vandenbunder, V. Fafeur, The multisubstrate docking site of the MET receptor is dispensable for MET-mediated RAS signaling and cell scattering, Mol. Biol. Cell 10 (1999) 551–565.
[32] S. Sano, S. Itami, K. Takeda, M. Tarutani, Y. Yamaguchi, H. Miura, K. Yoshikawa, S. Akira, J. Takeda, Keratinocyte-specific ablation of Stat3 exhibits impaired skin remodeling, but does not affect skin morphogenesis, EMBO J. 18 (1999) 4657–4668.
[33] Y. Ando, P.J. Jensen, Epidermal growth factor and insulin-like growth factor I enhance keratinocyte migration, J. Invest. Dermatol. 100 (1993) 633–639.

In Vitro Keratinocyte Dissociation Assay for Evaluation of the Pathogenicity of Anti-Desmoglein 3 IgG Autoantibodies in Pemphigus Vulgaris

Ken Ishii,*†[1] Reiko Harada,† Itsuro Matsuo,‡ Yuji Shirakata,§ Koji Hashimoto,§ and Masayuki Amagai*
*Department of Dermatology, Keio University School of Medicine, Tokyo, Japan; †Dermatology, Tokyo Electric Power Company Hospital, Tokyo, Japan; ‡Department of Dermatology, Teikyo University Ichihara Hospital, Ichihara, Japan; §Department of Dermatology, Ehime University School of Medicine, Matsuyama, Japan

Patients with pemphigus vulgaris (PV) have circulating anti-desmoglein (Dsg) 3 immunoglobulin G (IgG) autoantibodies that induce blister formation. We developed an *in vitro* quantitative assay to evaluate the pathogenic strength of anti-Dsg3 IgG autoantibodies in blister formation. To obtain intercellular adhesion mediated dominantly by Dsg3, we used primary cultured normal human keratinocytes expressing low level of Dsg2 in the presence of exfoliative toxin A that specifically digests Dsg1. After incubation with various antibodies, monolayers released by dispase were subjected to mechanical stress by pipetting, and the number of cell fragments were counted. When anti-Dsg3 monoclonal antibodies (mAb) obtained from pemphigus model mice were tested, pathogenic AK23 mAb yielded significantly higher number of cell fragments than AK7 or AK20 non-pathogenic mAb. Dissociation scores, defined with AK23 mAb as the positive control, were significantly higher with active stage PV sera ($n = 10$, 77.4 ± 21.4) than controls ($n = 11$, 16.0 ± 9.6; $p = 0.003$). When pair sera obtained from 6 PV patients in active stage and in remission were compared, the dissociation scores reflected well the disease activity as those in active stage were four to 17 times higher than those in remission. When sera from different patients showing similar ELISA scores but different clinical severity were tested ($n = 6$), the dissociation scores with sera from severe disease activity were significantly higher than those with sera in remission. These findings indicate that this dissociation assay will provide a simple and objective biological method to measure the pathogenic strength of pemphigus autoantibodies.

Key words: autoantibody/cell adhesion/desmoglein/pemphigus vulgaris
J Invest Dermatol 124:939–946, 2005

Pemphigus vulgaris (PV) is an autoimmune disease characterized by suprabasal blisters on the skin and mucous membrane. Without appropriate treatment, the disease can become severe or even fatal because of loss of the epidermal barrier function, leading to loss of body fluids or secondary infection (Amagai, 2003). Patients with PV have circulating immunoglobulin G (IgG) autoantibodies directed against desmoglein (Dsg) 3, a transmembrane desmosomal glycoprotein that belongs to the cadherin class of calcium-dependent adhesion molecules (Amagai *et al*, 1991). Compelling evidence indicates that autoantibodies in PV play a primary pathogenic role in blister formation (Anhalt *et al*, 1982; Amagai *et al*, 1992; 1994).

Indirect immunofluorescence and/or ELISA are widely used to measure titers of circulating IgG autoantibodies in PV. There is a general correlation between titers of PV autoantibodies and disease activity when monitored in individual patients (Beutner *et al*, 1985; Ishii *et al*, 1997; Cheng *et al*, 2002). But, we sometimes see patients with severe disease despite low titers of anti-Dsg3 autoantibodies. Furthermore, some PV cases with high titers of anti-Dsg3 autoantibodies exhibit mild disease severity (Harman *et al*, 2001). Thus, ELISA scores do not necessarily provide absolute values for the disease severity, probably because ELISA detects simply the immunoreactivity of anti-Dsg3 IgG autoantibodies and does not directly measure the pathogenic activity in disruption of intercellular adhesion of keratinocytes.

It is well known that autoantibodies in patients with pemphigus are polyclonal (Futei *et al*, 2000; Sekiguchi *et al*, 2001). Recently, Tsunoda *et al* (2003) isolated several mouse monoclonal anti-Dsg3 antibodies from PV model mice and demonstrated that there is pathogenic heterogeneity among the anti-Dsg3 monoclonal antibodies (mAb). Some antibodies have potency of blistering inducing activity *in vivo*. On the other hand, for other anti-Dsg3 antibodies, the *in vivo* binding of IgG to Dsg3 is not sufficient to cause blistering. Together with the discrepancy between disease severity and autoantibody titers in some cases with PV, it is assumed that there is pathogenic heterogeneity of IgG sera

Abbreviations: Dsg, desmoglein; ETA, exfoliative toxin A; IgG, immunoglobulin G; mAb, monoclonal antibody; NHK, normal human epidermal keratinocytes; PV, pemphigus vulgaris

[1]Present address: Department of Dermatology, University of Pennsylvania School of Medicine, Philadelphia, PA.

among different pemphigus patients. That is, IgG autoantibodies in pemphigus sera may contain both sets of pathogenic and non-pathogenic autoantibodies. Therefore, it is important to assess the pathogenicity of pemphigus IgG autoantibodies to elucidate the molecular mechanism of blister formation in pemphigus.

A passive transfer of PV sera to neonatal mice is a well-established assay to assess the pathogenic ability to induce bullous formation of PV sera (Anhalt *et al*, 1982). In the assay, injection of concentrated IgG prepared from PV sera to neonatal mice can induce blisters on the neonatal skin. This assay, however, requires a large volume of sera to induce blister formation in the skin of mice. In addition, although a subjective scaling (0–4) of the extent of the blister formation can be used (Mahoney *et al*, 1999), the assay does not detect the pathogenic strength in a quantitative manner. To compare pathogenic strength among pemphigus sera, a more sensitive assay to detect pathogenic activity needs to be developed.

In this paper, we developed an *in vitro* dissociation assay using primary human epidermal keratinocytes to measure the pathogenic activity of anti-Dsg3 autoantibodies in PV sera. The assay not only showed the difference of pathogenic strength among PV sera with similar ELISA scores but also provided a valuable tool to dissect molecular mechanisms for the heterogeneity in the pathogenic strength of pemphigus autoantibodies.

Results

Expression pattern of Dsg isoform varies among keratinocytes Dsg consists of four isoforms, Dsg1–4 (Getsios *et al*, 2004). There is evidence that Dsg1 and Dsg3 have compensatory functions in intercellular adhesion when they are co-expressed in the same cells *in vivo* (Mahoney *et al*, 1999; Wu *et al*, 2000). To detect specific disruption of intercellular adhesion by anti-Dsg3 antibody, ideal cells would be the ones that express predominantly Dsg3 without co-expression of other Dsg isoforms. To address this issue, we first characterized the expression pattern of Dsg isoforms in various cultured cells. KU8 cells derived from penile squamous cell carcinoma (SCC) and A431 cells derived from vulva squamous carcinoma mainly expressed Dsg2, whereas they expressed Dsg3 at a low level and no detectable Dsg1 (Fig 1). The predominant expression of Dsg2 is also known in other cultured epithelial cell lines, such as HaCaT keratinocytes, SCC lines, MDCK, or A431 cells (Schafer *et al*, 1994; Denning *et al*, 1998; Ishii *et al*, 2001). In contrast, primary cultured normal human epidermal keratinocytes (NHK) express predominantly Dsg3 and Dsg1 with minimal expression of Dsg2 (Fig 1). The shift in Ca^{2+} concentration of culture medium to 1.2 mM did not change the predominant expression of Dsg1 and Dsg3 in NHK cells (Fig 1).

To further eliminate the Dsg1 expression, we used staphyloccocal exotoxin, exfoliative toxin A (ETA), which specifically digests Dsg1 as a serine protease (Amagai *et al*, 2000). The treatment of NHK cells with 0.5 μg per mL of ETA for 2 h was sufficient to eliminate most of the expression of Dsg1 (Fig 1). Thus, NHK cells in the presence of ETA will provide cells predominantly expressing Dsg3.

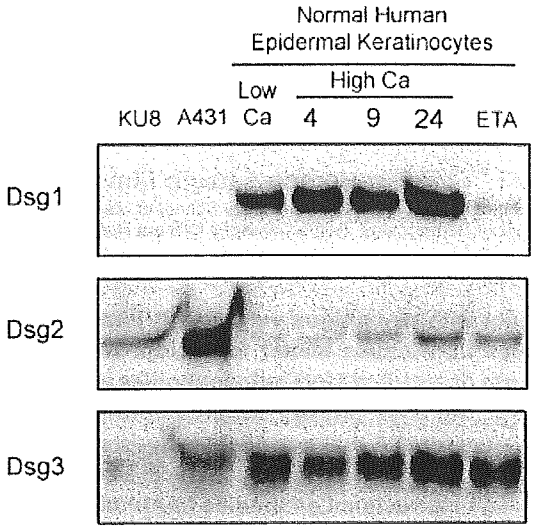

Figure 1
Expression pattern of desmoglein (Dsg) isoforms in cultured human epidermal keratinocytes. Normal human epidermal keratinocytes (NHK) were cultured to confluence in low-calcium medium and switched into 1.2 mM calcium-containing medium at 4, 9, or 24 h before harvest. In the exfoliative toxin A (ETA) lane, NHK were incubated with 0.5 μg per mL of ETA for 2 h after being cultured in high-calcium medium for 24 h. KU8 (squamous carcinoma cell line) and A431 (vulvar carcinoma cells) were also included. Total cell lysates were separated by 7.5% SDS-PAGE and subjected to immunoblot with antibodies against Dsg1 (982), Dsg2 (6D8), and Dsg3 (5H10). Note that NHK express Dsg3 and Dsg1 predominantly whereas KU8, and A431 cells express Dsg2 mainly.

Dsg3 dominant cell–cell adhesion is obtained by NHK cells in the presence of ETA To evaluate the intercellular adhesion of keratinocytes, we developed *in vitro* dissociation assay with modification of a previously described similar assay (Calautti *et al*, 1998; Caldelari *et al*, 2001; Huen *et al*, 2002). NHK cells cultured in 1.2 mM calcium containing medium were incubated with various antibodies or sera. Keratinocyte sheets released by dispase were subjected to a mechanical stress by pippeting.

When NHK cells were incubated without any antibodies, the cell sheet was well maintained even after the physical stress by pipetting (Fig 2*A*). Then we tested the effect of anti-Dsg3 mAb, AK23, which was obtained from PV model mice and proved to be pathogenic and capable of inducing blister formation in mice (Tsunoda *et al*, 2003). When NHK cells were incubated with AK23 mAb alone, the cell sheet was fragmented but only at a minimal level (Fig 2*B*). When NHK cells were incubated with ETA alone, the cell sheet was fragmented, but again only at a minimal level (Fig 2*C*). But, when NHK cells were incubated together with AK23 mAb and ETA, the cell sheet was broken into numerous smaller pieces (Fig 2*D*). Therefore, cell–cell adhesion of NHK cells in our culture condition is mediated by Dsg1 and Dsg3, which are compensating each other. These findings indicate that Dsg3-dominant cell–cell adhesion was obtained by NHK cells in the presence of ETA.

In addition, when we used HaCaT cells under similar conditions instead of NHK, incubation of AK23 mAb and ETA together did not induce a significant dissociation (data not shown). This illustrates the importance of using cells that express a low level of Dsg2 in this assay.

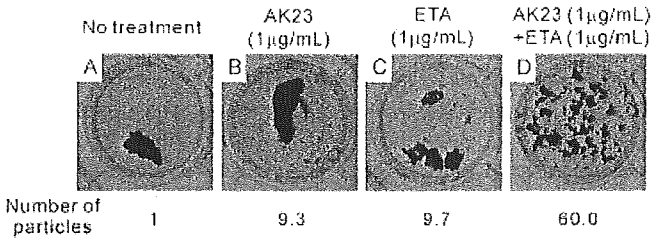

Figure 2
Treatment with combination of a pathogenic AK23 anti-desmoglein (Dsg) 3 monoclonal antibody and exfoliative toxin A (ETA)-dissociated cell sheets of normal human epidermal keratinocytes (NHK). Monolayers of NHK were treated with either AK23 monoclonal anti-Dsg3 antibody (1 μg per mL) overnight (*B*), ETA (1 μg per mL) for 2 h (*C*), or a combination of both reagents (*D*). Dissociation assay was performed as described in the Material and Methods section. Note that cell sheets were minimally dissociated when treated with only AK23 or ETA, whereas the cell sheets broke into numerous small fragments when treated with both AK23 and ETA. Numbers indicate a mean of numbers of fragments counted by image pro software using three captured images.

We could not evaluate the expression of Dsg4 (Kljuic *et al*, 2003; Whittock and Bower, 2003) because of unavailability of appropriate antibodies. But, the finding that the inactivation of Dsg3 by AK23 mAb and Dsg1 by ETA was sufficient to disrupt the cell–cell adhesion of NHK cells suggested that Dsg4 is either not expressed or, if expressed, Dsg4 may not play a significant role in cell adhesion at least in NHK cells.

Dissociation assay can detect pathogenic strength of anti-Dsg3 antibodies in disruption of intercellular adhesion To determine whether the dissociation assay using NHK cells was capable of evaluating different pathogenic activities among anti-Dsg3 IgG antibodies, we used AK series of mouse anti-Dsg3 mAb obtained from PV model mice (Tsunoda *et al*, 2003). The pathogenic activities of AK mAb had been determined by two *in vivo* assays: passive transfer using neonatal mice, and ascites formation using adult mice (Tsunoda *et al*, 2003). AK7 mAb does not cross-react with human Dsg3. AK20 mAb cross-reacts with human Dsg3, but does not induce apparent blisters by passive transfer assay or ascites formation assay. AK23 mAb, as mentioned above, induces blisters in the both assays.

Although cell sheets incubated with AK23 mAb were dissociated into numerous smaller fragments after a mechanical stress, cell sheets incubated with AK7 or AK20 mAb exhibited minimal dissociation as seen in untreated cell sheets (Fig 3*A*). The number of cell fragments revealed that AK23 mAb dissociated cell sheets 4.6–5.4-fold more than AK7 mAb. The number of cell particles treated with AK20 mAb was approximately the same as that of AK7 mAb, even though AK20 mAb has immunoreactivity against human Dsg3 (Fig 3*B*). In addition, shown in Fig 3*C*, the number of cell particles increased as the concentration of AK23 increased, indicating that this assay can detect pathogenic strength in a quantitative manner.

Thus, the dissociation assay using NHK cells in the presence of ETA could demonstrate the difference in the pathogenic activity among mouse anti-Dsg3 mAb.

Dissociation scores in PV were significantly higher than those of normal controls Next, we determined whether this assay reflects the pathogenic activity of human sera from PV patients. Ten sera from patients with PV in active stage and 11 normal individuals were analyzed by the dissociation assay (Fig 4). Of these 10 PV sera, five samples

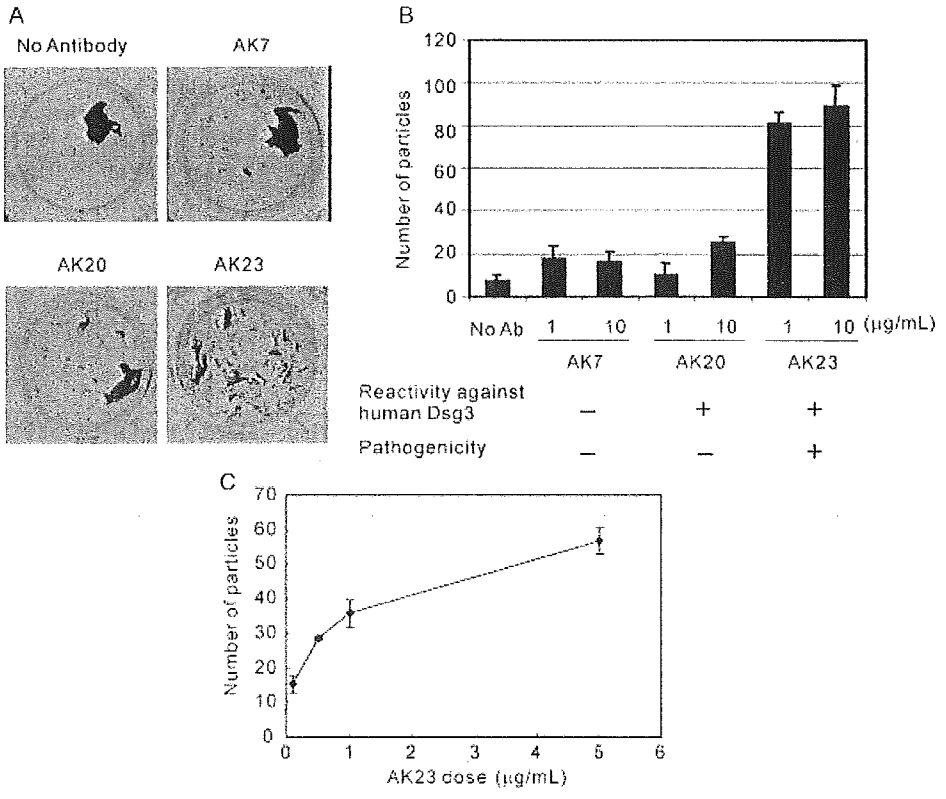

Figure 3
Dissociation assay to detect the pathogenic strength of anti-desmoglein (Dsg) 3 antibodies in disruption of intercellular adhesion. (*A*) Monolayers of normal human epidermal keratinocytes were treated with various monoclonal anti-Dsg3 antibodies. After 2 h incubation with 0.5 μg per mL of exfoliative toxin A, monolayers were separated from culture dishes by incubation with dispase. Subsequently, they were subjected to mechanical stress by pipetting using 1 mL of pipetman five times. AK7 does not have cross-reactivity with human Dsg3 and was used as a negative control. AK20 has reactivity against human Dsg3, but failed to induce apparent blisters by passive transfer to neonatal mice. AK23 has reactivity against human Dsg3 and has a pathogenic activity shown by passive transfer to neonatal mice. (*B*) Quantification was obtained by counting the number of fragments of cell sheets as described in the Material and Methods section. (*C*) The cell sheets were incubated with AK23 at concentrations of 0.1, 0.5, 1, and 5 μg per mL. Each condition was in duplicate. Bars represent standard deviations.

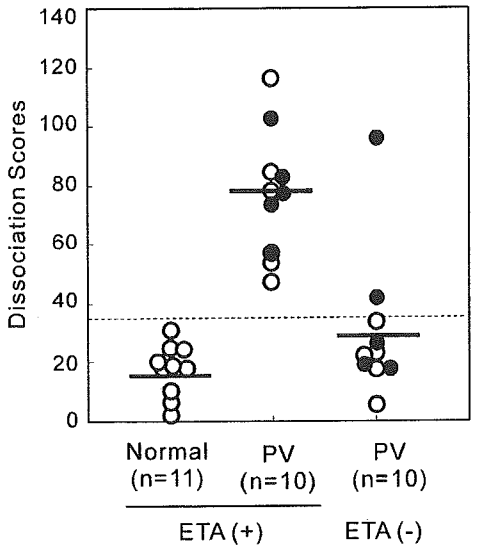

Figure 4
Dissociation assay to detect pathogenic activity in disruption of intercellular adhesion of pemphigus vulgaris (PV) sera. Ten sera patients with PV in active stage (five sera that have only anti-desmoglein (Dsg) 3 autoantibody (*open circle*) and five sera that have both Dsg3 and Dsg1 autoantibodies (*filled dot*)) and 11 sera from normal healthy controls were examined by the dissociation assay treated with and without exfoliative toxin A (ETA). A dashed line indicates a cut-off value, defined as an average plus 2 SD of normal control sera. Bars indicate averages of each group of samples. The dissociation scores of PV sera were significantly higher than that of normal controls (Mann–Whitney *U* test, $p = 0.003$). In the assay without treatment of ETA, the dissociation scores for PV sera were negative except two samples, which contain Dsg1 in addition to Dsg3 autoantibodies.

have anti-Dsg1 in addition to anti-Dsg3 antibodies. Confluent NHK sheets were incubated with the sera at a dilution of 1:5 for 24 h and treated with ETA for the last 2 h, and subsequently subjected to the dissociation assay. The dissociation scores were used to normalize interassay variability using the number of fragmented particles obtained by AK23 mAb as a positive control. A cut-off value was defined as the average value plus 2 SD of normal control sera. The mean of normal control sera was 16.0 ± 9.6, resulting in 35.2 as a cut-off value. None of the normal control sera fell above the cut-off value, whereas all of pemphigus sera exceeded the cut-off value. The dissociation scores with pemphigus sera range from 47.3 to 116.4 (mean $\pm$ SD $= 77.4 \pm 21.4$), which is significantly higher than those of normal control sera (Mann–Whitney *U* test, $p = 0.003$). These results suggest that this assay provides a tool to quantify the pathogenic strength of patients' sera in disruption of cell–cell adhesion.

When the PV sera samples were analyzed without ETA treatment, the dissociation scores of most samples were negative (Fig 4). The two PV sera that remained positive contained both anti-Dsg3 and anti-Dsg1 autoantibodies. Some PV sera contain anti-Dsg1 IgG autoantibodies, whereas others do not. Thus, the inactivation of Dsg1 by ETA is essential to determine the sole pathogenic strength of anti-Dsg3 IgG autoantibodies by eliminating the effects on dissociation of anti-Dsg1 IgG autoantibodies.

Dissociation scores correlate well with the clinical disease activity in PV We then determined whether the dissociation scores correlate well with the clinical disease activity in PV. We examined serum samples both during an active stage and in remission, which were obtained from two patients with mucocuaneous-type PV and four patients with mucosal dominant-type PV (Table I and Fig 5). The samples were analyzed by Dsg3 and Dsg1 ELISA as well.

Table I. Correlation of dissociation scores and clinical disease severity in PV

	Age (y)	Sex	Diagnosis	Clinical disease activity	Duration	ELISA		Dissociation scores	Initial treatment
						Dsg3	Dsg1		
Pt. 1	40	Male	PV-mc	Severe	3 y	1515.9	57.9	106.0	PSL 60 mg per d + plasmapheresis
				Remission		32.4	0.3	6.0	
Pt. 2	63	Male	PV-mc	Severe	5 mo	369.1	7.6	72.9	Methylprednisolone pulse +
				Remission		29.7	0	18.2	PSL 60 mg per d
Pt. 3	33	Male	PV-m	Severe	4 mo	514.9	1.2	180.0	PSL 60 mg + plasmapheresis
				Remission		73.2	0.1	30.0	
Pt. 4	47	Female	PV-m	Severe	10 mo	2553.7	4.8	111.1	PSL 40 mg per d
				Remission		5.7	0.3	28.7	
Pt. 5	35	Female	PV-m	Severe	2 y	443.3	1.9	143.4	Topical steroid application
				Remission		415.8	2.5	31.0	
Pt. 6	52	Male	PV-m	Severe	1 y	77.8	6.8	129.1	PSL 60 mg per d
				Remission		111	0.1	14.3	

PV-mc and PV-m indicate mucocutaneous type pemphigus vulgaris and mucosal dominant type pemphigus vulgaris, respectively.
Age is at patient's first presentation at hospital.
Dsg3 ELISA indicates the value obtained by multiplying the index value by dilution factor.
Dsg, desmoglein.

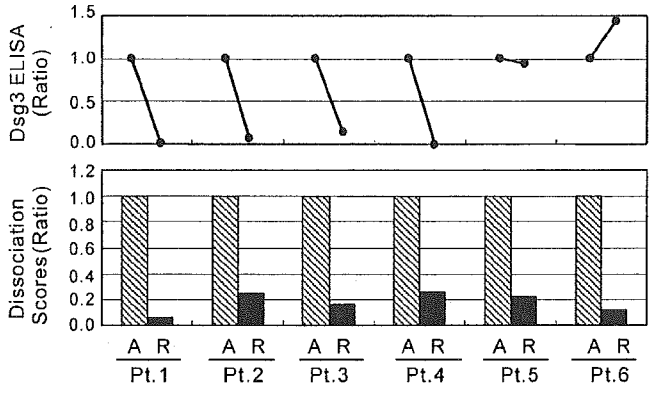

Figure 5
Dissociation scores correlate well with the clinical disease severity in pemphigus vulgaris (PV). Two mucocutaneous-type PV (Pt. 1 and 2) and four mucosal dominant-type PV (Pt. 3–6) were studied using *in vitro* dissociation assay and desmoglein (Dsg) 3 ELISA. Serum samples were taken when patients were in an active stage and in remission. Ratio of values to those in an active stage was shown for Dsg3 ELISA and *in vivo* dissociation assay. "A" and "R" represent an active stage and remission, respectively.

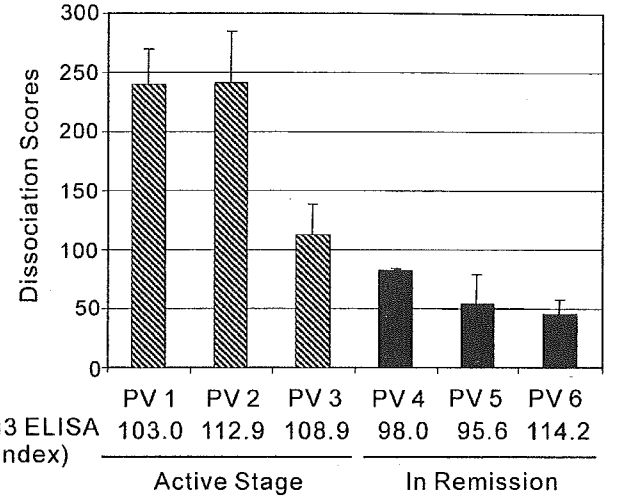

Figure 6
Detection of pathogenic heterogeneity of anti-desmoglein (Dsg) 3 autoantibodies in pemphigus vulgaris (PV) sera. Serum samples from six PV patients that have similar reactivity against Dsg3 were examined by dissociation assay (approximately 100 index in Dsg3 ELISA). Three of these samples were collected when the patients were in active stage. Three samples were collected when the patients were in remission.

In Pt. 1–4, Dsg3 ELISA scores were high at active stages and decreased in remission. In these patients, the dissociation scores also reflected the disease activity and showed high scores (72–180) at active stage and low scores (6–30) in remission. ELISA scores, however, sometimes fail to reflect the disease activity as seen in Pt. 5 and 6. In these patients, the ELISA scores in remission were about the same or even slightly higher than at active stages. Interestingly, even in these patients, the dissociation scores properly reflected the disease activity and showed high scores (143, 129) at the active stage and low scores (31, 14) in remission. Thus, the dissociation assay properly reflects the clinical disease activity within single patients.

Dissociation assay properly evaluates the disease activity among different patients with similar ELISA scores We finally examined whether the dissociation assay detects a pathogenic heterogeneity among PV sera from different patients. To address this, we selected serum samples from six PV patients who had similar Dsg3 ELISA scores but different disease activity (Fig 6). The ELISA index values of these six samples were approximately 100; three of them were from patients in the active stage, and three were from patients in remission. Despite the similar ELISA scores, the dissociation assay showed high scores (112–240) for those in an active stage and low scores for those in remission (44–82). These data suggest that this assay properly evaluates the pathogenic strength in blocking cell adhesion of PV sera and may provide the absolute indicator for the disease activity in PV.

Discussion

In this study, we developed an *in vitro* dissociation assay using cultured normal human keratinocytes. To characterize this assay, we first used a series of monoclonal anti-Dsg3 antibodies, which were isolated from pemphigus model mice and in which pathogenic activities were well characterized by means of *in vivo* pathogenicity assays. Pathogenic activities assessed from this *in vitro* assay reported here correlated with the data from the *in vivo* pathogenicity assays, suggesting that this assay was reliable in detecting the strength of anti-Dsg3 antibodies in disruption of intercellular adhesion. Next, when 10 PV sera and 11 normal control sera were analyzed, the dissociation scores in the PV sera group were significantly higher than those in normal controls, indicating that this assay can be used to measure the pathogenicity of pemphigus sera. The dissociation scores correlated with the disease severity in all six patients when analyzed with sera from different stages in individual patients. In addition, when we analyzed sera from different patients with similar immunoreactivity against Dsg3, the dissociation scores correlated well with clinical disease activity. These findings suggest that this assay may be useful to monitor the disease activity in pemphigus.

Although there may be a concern that pipetting cell sheets does not give a uniform stress, we did find that sheets without pathogenic antibodies were quite resistant to breakage and those with pathogenic antibodies were easily dissociated. Therefore, the amount of stress is probably not the critical factor in how well these sheets break up, at least within the range of stress generated by pipetting. Furthermore, dissociation by pipetting is a previously described technique used by several groups for this assay (Calautti *et al*, 1998; Caldelari *et al*, 2001). An alternative method for mechanical stress is rotation or shaking of tubes containing dispase-released cell sheets (Huen *et al*, 2002; Setzer *et al*, 2004). We found that the stress by rotation was too mild to reproducibly induce dissociation in our condition. Therefore, we chose pipetting to provide mechanical stress to cell sheets and the results demonstrate that the assay, as performed, does correlate well with disease activity.

This assay can detect the strength of intercellular adhesion disruption only for anti-Dsg3 antibodies. This was made possible because we used primary human keratinocytes with low expression of Dsg2 and used ETA to digest Dsg1, which results in the culture cells mainly expressing Dsg3. It was shown that Dsg1 and Dsg3 compensate each other in their adhesive function in epithelial cells *in vivo* (Mahoney *et al*, 1999; Wu *et al*, 2000). If isoforms other than Dsg3 were expressed in the same cells, it was assumed that the isoforms mask the disruption effect of cell adhesion by Dsg3 antibody. The human keratinocytes we used here expressed both Dsg3 and Dsg1 predominantly. When keratinocyte sheets were incubated only with monoclonal anti-Dsg3 antibodies, the cell sheets were not dissociated well. When the keratinocytes were incubated both with monoclonal Dsg3 antibodies and ETA, the cell sheets were dissociated. This finding is further evidence to support the hypothesis that Dsg isoforms compensate for each other in their adhesive function.

To evaluate the disease activity of pemphigus, titers obtained from indirect immunofluorescence or ELISA are currently used. In general, the titers fluctuate in parallel with disease severity when monitored in a single individual. In some cases, however, values of Dsg3 ELISA remain high although the disease is clinically inactive (Harman *et al*, 2001). Creswell *et al* (1981) studied 21 cases of pemphigus regarding the correlation of disease activity and serial titers of indirect immunofluorescence. They found that in one case of 21 cases, the titer remained elevated in spite of clinical remission. Pt. 5 and 6 in Table I are examples of such cases. Despite a high value of Dsg3 ELISA, the dissociation scores in these cases were low during clinical remission. This could be explained by the fact that ELISA or immunofluorescence is a serological assay to detect binding capacity against Dsg3 by autoantibodies. Compared with this, the dissociation assay is a biological assay to detect the cell adhesive strength. The values from this dissociation assay directly show the pathogenic strength of autoantibodies in intercellular adhesion. This is useful for evaluation of the disease severity for pemphigus.

We have shown that sera with the same immunoreactivity against Dsg3 have different properties in disruption of cell adhesion (Fig 6). This demonstrates that sera have heterogeneous properties in blocking of intercellular adhesion. This finding raised the question as to what the determinants of pathogenicity of autoantibodies in pemphigus sera are. One possible explanation as to what determines pathogenicity of autoantibodies is epitopes that autoantibodies bind. There is some evidence that pemphigus sera target multiple epitopes on Dsg1 and Dsg3 molecules (Futei *et al*, 2000; Sekiguchi *et al*, 2001). Tsunoda *et al* isolated eight monoclonal anti-Dsg3 antibodies that have different properties in disruption of intercellular adhesion. The epitope of a pathogenic antibody Ak23 was mapped in the region of the adhesive interface between juxtaposed Dsg3, whereas the epitope of mAb that failed to induce apparent pathogenic activity was mapped in the middle to carboxyl terminal extracellular region, where no direct intermolecular interaction was predicted. Another paper showed that in endemic pemphigus foliaceus (FS), another type of pemphigus characterized by anti-Dsg1 autoantibodies, disease onset was associated with the emergence of autoantibodies specific for epitopes in the amino-terminal domain. In addition, sera from FS patients in remission showed reactivity restricted to carboxyl terminal extracellular region (Li *et al*, 2003). Thus, it is possible that the binding epitopes may determine pathogenic activities. Alternatively, it is possible that a combination of several autoantibodies against different epitopes may induce strong pathogenicity, although a single individual autoantibody itself does not have strong pathogenic activity. As the dissociation assay is a simplified and sensitive test to detect pathogenicity of anti-Dsg3 autoantibodies, a combination of epitope mapping and this dissociation assay would be helpful to determine the pathogenic factor on Dsg3 molecules.

In summary, we developed a dissociation assay to detect the pathogenic strength of Dsg3 antibodies in disruption of intercellular adhesion. The dissociation assay provides a useful tool to evaluate the pathogenic strength of pemphigus autoantibodies. Furthermore, the evaluation of the pathogenic strength of pemphigus autoantibodies will provide us with a better understanding for what defines the pathogenic heterogeneity among anti-Dsg3 autoantibodies in pemphigus.

Material and Methods

Human sera PV is subdivided into two types: mucosal dominant type and mucocutaneous type. Mucosal-type PV have only anti-Dsg3 autoantibodies whereas mococutaneous-type PV have anti-Dsg3 and Dsg1 autoantibodies (Ishii *et al*, 1997; Amagai *et al*, 1999b). Sera were obtained from 10 patients with PV, whose diagnoses were confirmed by clinical, histologic, and immunopathological findings. Of these samples, five sera had anti-Dsg1 in addition to anti-Dsg3 autoantibodies determined by Dsg ELISA. For analysis of correlation between disease activity and dissociation scores, serum samples were collected from another six PV patients at active stage and in remission. Of these samples, we included two cases with high scores of Dsg3 ELISA even in remission (Pt. 5 and 6 in Table I). In addition, for analysis of pathogenic heterogeneity among sera from different PV patients, another six samples with similar Dsg3 ELISA scores but different disease activity were selected. The study was approved by the institution review board of Keio University and was conducted according to the Declaration of Helsinki Principles. All samples were used with informed consent.

Antibodies AK series of mouse AK7, AK20, and AK23 mAb against mouse and human Dsg3 were prepared as previously described (Tsunoda *et al*, 2003). The following mouse mAb were used for immunoblots: 6D8, against Dsg2 (a kind gift from Dr M. Wheelock (Wahl *et al*, 1996)), and 5H10, against human Dsg3 (Proby *et al*, 2000). Serum from a patient with pemphigus follaceus was also used to detect Dsg1.

Cell culture NHK were obtained and cultured in medium MDCB153 as described before (Shirakata *et al*, 2003). KU8 cells isolated from a penile squamous cell line, and A431 cells were cultured in DMEM with 10% fetal bovine serum (Tsukamoto, 1989; Ishii *et al*, 2001). The human naturally immortalized keratinocyte HaCaT cell line was a kind gift from Dr Norbert Fusenig (German Cancer Research Center, Heidelberg, Germany) and cultured in DMEM with 10% fetal bovine serum.

Production of recombinant ETA Recombinant ETA with His tag on the carboxyl terminal end was expressed in *Escherichia coli* DH10B (Yamaguchi *et al*, 2002) and recovered from the soluble

fraction in lysis buffer (20 mM Tris-HCl (pH 8.0), 0.2 M NaCl, 0.2% Triton X-100, and protease inhibitor cocktail (Complete Mini, EDTA free; Roche Diagnostics, Mannheim, Germany)), and purified with TALON affinity resin (Clontech, Palo Alto, California).

Development of dispase-based dissociation assay NHK cells were seeded onto 12-well plates and cultured in MDCB153 medium containing 0.1 mM calcium. After reaching confluency, the medium was changed to the one with 1.2 mM calcium. Various antibodies or sera were added and incubated at 37°C overnight. Two hours before the assay, the cells were incubated with ETA at 0.5 μg per mL to cleave Dsg1 specifically (Amagai *et al*, 2000). After washing with PBS twice, NHK were incubated with dispase (Roche Diagnostics) for 15 min to release cells as monolayers. Released monolayers were carefully washed with PBS twice and subject to mechanical stress by pipetting with a 1 mL pipetman. Fragments were fixed by adding formaldehyde at a final concentration of 3% and stained by adding crystal violet (Sigma-aldrich, St Louis, Missouri). The number of particles was determined as an average of the number of cell particles counted by image pro software (Media Cybernetics, Silver Spring, Maryland), using three sets of images captured by a digital camera for each plate. Dissociation scores were calculated using the number of fragmented cell sheets (N) using the following formula: Dissociation scores = ((N with serum − N without serum)/(N with AK23 − N without serum)) × 100. The cell sheet with AK23 at 1 μg per mL was included in each assay to adjust for interassay variability.

Immunoblot analyses Cells were lyzed in 2 × Laemmli SDS-sample buffer and the concentration of each sample was measured by an amido black protein assay (Sheffield *et al*, 1987). Equal volume of samples was size-fractionated by SDS-PAGE and transferred to an Immobilon- P membrane (Millipore, Bedford, Massachusetts). Antibodies were used at the following dilutions for immunoblots: PF serum (#982, a kind gift from Dr John R. Stanley) against Dsg1, 1:1000; 6D8 against Dsg2, 1:1000; and 5H10 against Dsg3, 1:1000. A peroxidase-conjugated anti-mouse IgG antibody (Medical and Biological Laboratories, Nagoya, Japan) and a peroxidase-linked anti-human Ig antibody (Amersham, Uppsala, Sweden) were used as secondary antibodies.

Dsg3 and Dsg1 ELISA Immunoreactivity against Dsg3 and Dsg1 of IgG autoantibodies in PV sera was analyzed by Dsg3 and Dsg1 ELISA following the manufacture's instructions (Medical and Biological Laboratories) (Ishii *et al*, 1997; Amagai *et al*, 1999a). When the ELISA index values were greater than 150, the sera were serially diluted from 1:100 to 1:1600 to determine the optimal dilution, and the "true" index values were obtained by multiplying the index values by the dilution factor (Cheng *et al*, 2002).

Statistics The Mann–Whitney *U* test was used for comparison of dissociation scores between PV sera and normal controls.

We would like to thank Dr Takeji Nishikawa for insightful discussion, and Drs Kathleen Green and Arthur Huen for their valuable advice. We also thank Dr M. Wheelock for 6D8 mAb, Dr John R.Stanley for #982 PF serum, and Dr Norbert Fusenig for HaCaT cells. Additionally, we thank Ms Minae Suzuki for performing the ELISA. This work was supported by Health and Labour Sciences Research Grants for Research on Measures for Intractable Diseases, from the Ministry of Health, Labor, and Welfare, and by Grants-in-Aid for Scientific Research from the Ministry of Education, Culture, Sports, Science, and Technology of Japan.

DOI: 10.1111/j.0022-202X.2005.23714.x

Manuscript received November 04, 2004; revised December 03, 2004; accepted for publication January 10, 2005

Address correspondence to: Ken Ishii, MD, PhD, Department of Dermatology, Keio University School of Medicine, 35 Shinanomachi, Shinjuku-Ku, Tokyo 160-8582, Japan. Email: ken4ishii@aol.com

References

Amagai M: Desmoglein as a target in autoimmunity and infection. J Am Acad Dermatol 48:244–252, 2003

Amagai M, Hashimoto T, Shimizu N, Nishikawa T: Absorption of pathogenic autoantibodies by the extracellular domain of pemphigus vulgaris antigen (Dsg3) produced by baculovirus. J Clin Invest 94:59–67, 1994

Amagai M, Karpati S, Prussick R, Klaus-Kovtun V, Stanley JR: Autoantibodies against the amino-terminal cadherin-like binding domain of pemphigus vulgaris antigen are pathogenic. J Clin Invest 90:919–926, 1992

Amagai M, Klaus-Kovtun V, Stanley JR: Autoantibodies against a novel epithelial cadherin in pemphigus vulgaris, a disease of cell adhesion. Cell 67: 869–877, 1991

Amagai M, Komai A, Hashimoto T, *et al*: Usefulness of enzyme-linked immunosorbent assay (ELISA) using recombinant desmoglein 1 and 3 for serodiagnosis of pemphigus. Br J Dermatol 140:351–357, 1999a

Amagai M, Matsuyoshi N, Wang ZH, Andl C, Stanley JR: Toxin in bullous impetigo and staphylococcal scalded-skin syndrome targets desmoglein 1. Nat Med 6:1275–1277, 2000

Amagai M, Tsunoda K, Zillikens D, Nagai T, Nishikawa T: The clinical phenotype of pemphigus is defined by anti-desmoglein autoantibody profile. J Am Acad Dermatol 40:167–170, 1999b

Anhalt GJ, Labib RS, Voorhees JJ, Beals TF, Diaz LA: Induction of pemphigus in neonatal mice by passive transfer of IgG from patients with the disease. N Engl J Med 306:1189–1196, 1982

Beutner EH, Chorzelski TP, Jablonska S: Immunofluorescence tests: Clinical significance of sera and skin in bullous diseases. Int J Dermatol 24: 405–421, 1985

Calautti E, Cabodi S, Stein PL, Hatzfeld M, Kedersha N, Paolo Dotto G: Tyrosine phosphorylation and src family kinases control keratinocyte cell–cell adhesion. J Cell Biol 141:1449–1465, 1998

Caldelari R, de Bruin A, Baumann D, Suter MM, Bierkamp C, Balmer V, Muller E: A central role for the armadillo protein plakoglobin in the autoimmune disease pemphigus vulgaris. J Cell Biol 153:823–834, 2001

Cheng SW, Kobayashi M, Kinoshita-Kuroda K, Tanikawa A, Amagai M, Nishikawa T: Monitoring disease activity in pemphigus with enzyme-linked immunosorbent assay using recombinant desmogleins 1 and 3. Br J Dermatol 147:261–265, 2002

Creswell SN, Black MM, Bhogal B, Skeete MV: Correlation of circulating intercellular antibody titres in pemphigus with disease activity. Clin Exp Dermatol 6:477–483, 1981

Denning MF, Guy SG, Ellerbroek SM, Norvell SM, Kowalczyk AP, Green KJ: The expression of desmoglein isoforms in cultured human keratinocytes is regulated by calcium, serum, and protein kinase C. Exp Cell Res 239: 50–59, 1998

Futei Y, Amagai M, Sekiguchi M, Nishifuji K, Fujii Y, Nishikawa T: Use of domain-swapped molecules for conformational epitope mapping of desmoglein 3 in pemphigus vulgaris. J Invest Dermatol 115:829–834, 2000

Getsios S, Huen AC, Green KJ: Working out the strength and flexibility of desmosomes. Nat Rev Mol Cell Biol 5:271–281, 2004

Harman KE, Seed PT, Gratian MJ, Bhogal BS, Challacombe SJ, Black MM: The severity of cutaneous and oral pemphigus is related to desmoglein 1 and 3 antibody levels. Br J Dermatol 144:775–780, 2001

Huen AC, Park JK, Godsel LM, *et al*: Intermediate filament-membrane attachments function synergistically with actin-dependent contacts to regulate intercellular adhesive strength. J Cell Biol 159:1005–1017, 2002

Ishii K, Amagai M, Hall RP, *et al*: Characterization of autoantibodies in pemphigus using antigen-specific enzyme-linked immunosorbent assays with baculovirus-expressed recombinant desmogleins. J Immunol 159: 2010–2017, 1997

Ishii K, Norvell SM, Bannon LJ, Amargo EV, Pascoe LT, Green KJ: Assembly of desmosomal cadherins into desmosomes is isoform dependent. J Invest Dermatol 117:26–35, 2001

Kljuic A, Bazzi H, Sundberg JP, *et al*: Desmoglein 4 in hair follicle differentiation and epidermal adhesion: Evidence from inherited hypotrichosis and acquired pemphigus vulgaris. Cell 113:249–260, 2003

Li N, Aoki V, Hans-Filho G, Rivitti EA, Diaz LA: The role of intramolecular epitope spreading in the pathogenesis of endemic pemphigus foliaceus (fogo selvagem). J Exp Med 197:1501–1510, 2003

Mahoney MG, Wang Z, Rothenberger K, Koch PJ, Amagai M, Stanley JR: Explanations for the clinical and microscopic localization of lesions in pemphigus foliaceus and vulgaris. J Clin Invest 103:461–468, 1999

Proby CM, Ota T, Suzuki H, *et al*: Development of chimeric molecules for recognition and targeting of antigen-specific B cells in pemphigus vulgaris. Br J Dermatol 142:321–330, 2000

Schafer S, Koch PJ, Franke WW: Identification of the ubiquitous human desmoglein, Dsg2, and the expression catalogue of the desmoglein subfamily of desmosomal cadherins. Exp Cell Res 211:391–399, 1994

Sekiguchi M, Futei Y, Fujii Y, Iwasaki T, Nishikawa T, Amagai M: Dominant autoimmune epitopes recognized by pemphigus antibodies map to the N-terminal adhesive region of desmogleins. J Immunol 167:5439–5448, 2001

Setzer SV, Calkins CC, Garner J, Summers S, Green KJ, Kowalczyk AP: Comparative analysis of armadillo family proteins in the regulation of a431 epithelial cell junction assembly, adhesion and migration. J Invest Dermatol 123:426–433, 2004

Sheffield JB, Graff D, Li HP: A solid-phase method for the quantitation of protein in the presence of sodium dodecyl sulfate and other interfering substances. Anal Biochem 166:49–54, 1987

Shirakata Y, Tokumaru S, Yamasaki K, Sayama K, Hashimoto K: So-called biological dressing effects of cultured epidermal sheets are mediated by the production of EGF family, TGF-beta and VEGF. J Dermatol Sci 32:209–215, 2003

Tsukamoto T: Establishment and characterization of a cell line (KU-8) from squamous cell carcinoma of the penis. Keio J Med 38:277–293, 1989

Tsunoda K, Ota T, Aoki M, *et al*: Induction of pemphigus phenotype by a mouse monoclonal antibody against the amino-terminal adhesive interface of desmoglein 3. J Immunol 170:2170–2178, 2003

Wahl JK, Sacco PA, McGranahan-Sadler TM, Sauppe LM, Wheelock MJ, Johnson KR: Plakoglobin domains that define its association with the desmosomal cadherins and the classical cadherins: Identification of unique and shared domains. J Cell Sci 109:1143–1154, 1996

Whittock NV, Bower C: Genetic evidence for a novel human desmosomal cadherin, desmoglein 4. J Invest Dermatol 120:523–530, 2003

Wu H, Wang ZH, Yan A, *et al*: Protection against pemphigus foliaceus by desmoglein 3 in neonates. N Engl J Med 343:31–35, 2000

Yamaguchi T, Nishifuji K, Sasaki M, *et al*: Identification of the *Staphylococcus aureus* etd pathogenicity island which encodes a novel exfoliative toxin, ETD, and EDIN-B. Infect Immun 70:5835–5845, 2002

2 Leow YH, Soon YH, Tham SN. A report of 31 cases of porokeratosis at the National Skin Centre. *Ann Acad Med Singapore* 1996; **25**:837–41.
3 Sasson M, Krain AD. Porokeratosis and cutaneous malignancy. A review. *Dermatol Surg* 1996; **22**:339–42.
4 Goerttler EA, Jung EG. Porokeratosis and skin carcinoma: a critical review. *Humangenetik* 1975; **26**:291–6.
5 Otsuka F, Someya T, Ishibashi Y. Porokeratosis and malignant skin tumours. *J Cancer Res Clin Oncol* 1991; **117**:55–60.
6 Dos Reis Gadelha A, Espirito Santo De Campos Z, Figueiredo Barreto RA. Mibelli's porokeratosis and basaloid epithelioma. *Med Cutan Ibero Lat Am* 1984; **12**:117–21.
7 Patrizi A, Passarini B, Minghetti G, Masina M. Porokeratosis palmaris et plantaris disseminata: an unusual clinical presentation. *J Am Acad Dermatol* 1989; **21**:415–18.
8 Roson E, Garcia-Doval I, De La Torre C *et al.* Disseminated superficial porokeratosis with mucosal involvement. *Acta Derm Venereol (Stockh)* 2001; **81**:64–5.
9 Otsuka F, Shima A, Ishibashi Y. Porokeratosis as a premalignant condition of the skin. Cytologic demonstration of abnormal DNA ploidy in cells of the epidermis. *Cancer* 1989; **63**:891–6.
10 Bencini PL, Tarantino A, Grimalt R *et al.* Porokeratosis and immunosuppression. *Br J Dermatol* 1995; **132**:74–8.

Conflicts of interest: none declared.

Cre-loxP adenovirus-mediated foreign gene expression in skin-equivalent keratinocytes

DOI: 10.1111/j.1365-2133.2005.06637.x

SIR, The introduction of genes into normal human cells is a fundamental component of human gene therapy.[1] Normal human keratinocytes (NHK) are appropriate targets for gene therapy[2] because of the accessibility of the epidermis and the possibility of excising genetically modified NHK sheets from recipient skin in cases of adverse reaction. From the gene therapy safety point of view, regulated expression of introduced genes is an important consideration.[3] The Cre-loxP system is one of the most reliable gene regulation systems used in gene targeting in virus vectors.[4] We used this system in a novel way to express genes at high levels in skin-equivalent NHK.

In preliminary experiments, NHK in monolayer cultures were infected with adenovirus (Ad) and seeded on to a collagen gel. Although enhanced green fluorescent protein (EGFP) expression was detected in the epidermal sheet, the expression was mainly in the cornified layer and only weak expression was seen in the basal and spinous layers (data not shown). Therefore, we modified the method to obtain more efficient gene expression (Fig. 1). The epidermal sheet was removed from the collagen gel

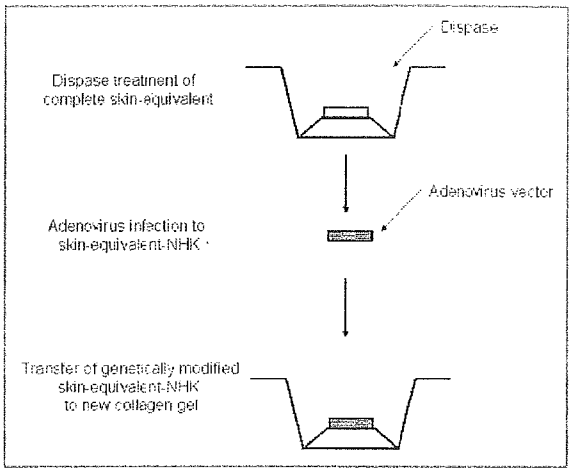

Fig 1. Experimental scheme of adenovirus (Ad) infection for shuttle-transduced skin equivalents. In the shuttle–skin equivalent method, completed skin-equivalent normal human keratinocyte (NHK) sheets were removed from the collagen gel by dispase treatment, infected with Ad, then seeded on a new collagen gel and incubated for 48 h.

once the skin equivalent had formed and was infected with the Ad; it was then placed on a new collagen gel, which was incubated for 2–3 days. In the genetically modified skin equivalent, strong EGFP expression was seen in the basal and suprabasal layers, using confocal laser microscopy (Fig. 2).

Several reports have suggested the possibility of making tissue- or tumour-specific Ad vectors[5,6] incorporating chemically inducible gene expression, such as the Tet-on/Tet-off system. These vectors would be especially applicable to Ad-mediated gene regulation in skin after implanting genetically modified skin-equivalent epidermis where topical application of the inducer chemical is possible. The Ad Cre-loxP system is an efficient method of inserting genes and regulating their expression in NHK. With this technique, we are able to induce high-level expression of different genes and to develop disease models in which the involvement of individual mutated genes in disease pathogenesis and the efficacy of gene therapies could be studied. In the past, it was possible to express toxic genes in Ad vectors; however, the virus titres tended to be low. Using the Cre-loxP system, high-titre viruses containing toxic genes could be obtained (e.g. Fas-ligand[7]). Our goal is to contribute to the quality of life of patients by developing a new method to introduce target genes with high expression levels into skin-equivalent keratinocytes. Further experiments are needed to optimize target gene expression in NHK.

Acknowledgments

We thank Mr Kouichi Ukon, Ms Teruko Tsuda and Ms Akiko Kon for technical assistance. We also thank Dr Izumu Saitou (Tokyo, Japan) for the adenovirus expression system and

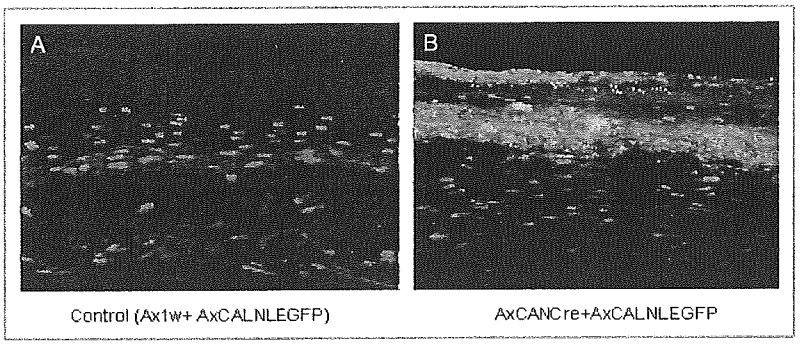

Fig 2. Confocal laser microscopic views of enhanced green fluorescent protein (EGFP) expression in shuttle–skin equivalent using the Cre-loxP adenovirus (Ad) system. (A) Control (Ax1w + AxCALNLEGFP); (B) AxCANCre + AxCALNLEGFP doubly infected shuttle-transduced skin equivalent. The cell nuclei were stained with propidium iodide. EGFP expression was detected at high levels in the basal and spinous cell layers when the Cre-loxP Ad system was used.

adenovirus Cre-loxP system and Dr Jun-ichi Miyazaki for the CAG promoter. This work was partly supported by Health Sciences Research Grants for Research on Specific Diseases from the Ministry of Health and Welfare and a Grant-in-Aid for Scientific Research from the Ministry of Education, Science and Culture of Japan.

Department of Dermatology,
Ehime University School of Medicine,
Shitukawa, Toon City 791–0295, Japan
E-mail: hanakawa@m.ehime-u.ac.jp

Y. Hanakawa
Y. Shirakata
H. Nagai
Y. Yahata
S. Tokumaru
K. Yamasaki
M. Tohyama
K. Sayama
K. Hashimoto

References

1 Verma IM, Somia N. Gene therapy – promises, problems and prospects. *Nature* 1997; **389**:239–42.
2 Vogel JC, Walker PS, Hengge UR. Gene therapy for skin diseases. *Adv Dermatol* 1996; **11**:383–98.
3 Miller N, Whelan J. Progress in transcriptionally targeted and regulatable vectors for genetic therapy. *Hum Gene Ther* 1997; **8**:803–15.
4 Kanegae Y, Takamori K, Sato Y *et al.* Efficient gene activation system on mammalian cell chromosomes using recombinant adenovirus producing Cre recombinase. *Gene* 1996; **181**:207–12.
5 Kaneko S, Hallenbeck P, Kotani T *et al.* Adenovirus-mediated gene therapy of hepatocellular carcinoma using cancer-specific gene expression. *Cancer Res* 1995; **55**:5283–7.
6 Morishita K, Johnson DE, Williams LT. A novel promoter for vascular endothelial growth factor receptor (flt-1) that confers endothelial-specific gene expression. *J Biol Chem* 1995; **270**:27948–53.
7 Okuyama T, Fujino M, Li XK *et al.* Efficient Fas-ligand gene expression in rodent liver after intravenous injection of a recombinant adenovirus by the use of a Cre-mediated switching system. *Gene Ther* 1998; **5**:1047–53.

Conflicts of interest: none declared.

Efficacy of issuing guidelines on acne management to general practitioners

DOI: 10.1111/j.1365-2133.2005.06641.x

Sir, The objective of this study was to evaluate the practice of issuing guidelines on acne management to general practitioners (GPs) in our region. Acne can be managed in a primary care setting with appropriate training and experience.[1] However, specialist referral is required for initiation of isotretinoin. An evaluation of random referrals prior to introduction of guidelines showed that significant numbers of referrals were not in accordance with established guidelines. We used the consensus guidelines issued by the National Institute for Clinical Excellence (NICE) December 2001 as a gold standard for referral to specialist centres and based our guidelines on these criteria. NICE guidelines advocate referral to a specialist service if any of the following circumstances apply: (i) a severe variant of acne such as acne fulminans or Gram-negative folliculitis; (ii) severe or nodulocystic acne; (iii) severe social or psychological problems; (iv) risk or presence of scarring despite primary care therapies; (v) moderate acne that has failed to respond to treatment that included two courses of oral antibiotics, each lasting 3 months; and (vi) a suspected underlying endocrinological condition (such as polycystic ovary syndrome) that warrants assessment.

We also issued recommendations to optimize antibiotic prescribing which were based on established guidelines.[2,3] For example, tetracycline or oxytetracycline 500 mg twice daily were suggested as the antibiotics of choice, as they are effective and inexpensive. Doxycycline 50 mg once daily was advised if there was poor compliance with first-line agents. It was advised to reserve minocycline[2,4] and erythromycin[2] for those who fail to respond to first-line agents. Simultaneous use of different topical and oral antibiotics was discouraged.[5]

Heparin-binding EGF-like growth factor accelerates keratinocyte migration and skin wound healing

Yuji Shirakata[1,*,‡], Rina Kimura[2,*], Daisuke Nanba[3], Ryo Iwamoto[2], Sho Tokumaru[1], Chie Morimoto[3], Koichi Yokota[4], Masanori Nakamura[4], Koji Sayama[1], Eisuke Mekada[2], Shigeki Higashiyama[3] and Koji Hashimoto[1]

[1]Department of Dermatology, Ehime University School of Medicine, Ehime 791-0295, Japan
[2]Research Institute for Microbial Diseases, Osaka University, Osaka 565-0871, Japan
[3]Biochemistry and Molecular Genetics, Ehime University School of Medicine, Ehime 791-0295, Japan
[4]Carna Biosciences Incorporated, Kobe, Hyogo 650-0047, Japan
*These authors contributed equally to this work
‡Author for correspondence (e-mail: shirakat@m.ehime-u.ac.jp)

Accepted 14 February 2005
Journal of Cell Science 118, 2363-2370 Published by The Company of Biologists 2005
doi:10.1242/jcs.02346

Summary

Members of the epidermal growth factor (EGF) family are the most important growth factors involved in epithelialization during cutaneous wound healing. Heparin-binding EGF-like growth factor (HB-EGF), a member of the EGF family, is thought to play an important role in skin wound healing. To investigate the in vivo function of HB-EGF in skin wound healing, we generated keratinocyte-specific HB-EGF-deficient mice using Cre/loxP technology in combination with the keratin 5 promoter. Studies of wound healing revealed that wound closure was markedly impaired in keratinocyte-specific HB-EGF-deficient mice. HB-EGF mRNA was upregulated at the migrating epidermal edge, although cell growth was not altered. Of the members of the EGF family, HB-EGF mRNA expression was induced the most rapidly and dramatically as a result of scraping in vitro. Combined, these findings clearly demonstrate, for the first time, that HB-EGF is the predominant growth factor involved in epithelialization in skin wound healing in vivo and that it functions by accelerating keratinocyte migration, rather than proliferation.

Key words: Conditional knockout, HB-EGF, Keratinocytes, Migration, Wound healing

Introduction

Cutaneous wound healing requires precise coordination of epithelialization, dermal repair and angiogenesis (Singer and Clark, 1999). Epithelialization is ultimately dependent on the migratory, proliferative and differentiation abilities of keratinocytes. The growth and differentiation of keratinocytes are regulated mainly by a variety of growth factors (Hashimoto, 2000), of which the members of the epidermal growth factor (EGF) family are the most important for skin wound healing.

The EGF family consists of EGF, transforming growth factor (TGF)-α, heparin binding EGF-like growth factor (HB-EGF), amphiregulin (AR), epiregulin (EPR), betacellulin (BTC), epigen and neuregulin (NRG)-1, NRG-2, NRG-3 and NRG-4 (Falls, 2003; Harari et al., 1999). The EGF receptor (EGFR) family consists of EGFR (also called ErbB1), ErbB2, ErbB3 and ErbB4 (Jorissen et al., 2003). The mammalian ligands that bind EGFR include EGF, HB-EGF, TGF-α, AR, BTC, EPR and epigen. Recent studies using gene targeting or transgenic models have revealed that EGFR is essential for epithelial development in the skin, lung and gastrointestinal tract, whereas ErbB2, ErbB3, ErbB4 and neuregulins are essential for the development of cardiac muscle and the central nervous system (Erickson et al., 1997; Gassmann et al., 1995; Lee et al., 1995; Meyer and Birchmeier, 1995; Miettinen et al., 1995; Murillas et al., 1995; Riethmacher et al., 1997; Sibilia and Wagner, 1995).

Previous reports have shown that TGF-α, AR, HB-EGF and EPR are autocrine growth factors in normal human epidermal keratinocytes (NHEK) (Coffey et al., 1987; Cook et al., 1991; Hashimoto et al., 1994; Shirakata et al., 2000). It has been reported that keratinocyte migration and proliferation are predominantly mediated by autocrine EGFR activation (Stoll et al., 1997). However, the importance of the role that the EGF family plays in skin wound healing has not been confirmed in vivo using knockout mice. Previously, Marikovsky et al. (Marikovsky et al., 1993) reported that HB-EGF is a major component of the mix of growth factors found in wound fluid. Therefore, we speculated that HB-EGF was an important member of the EGF family in cutaneous wound healing. To test this hypothesis, we generated keratinocyte-specific HB-EGF knockout mice, and clearly demonstrated that HB-EGF is an important growth factor for epithelialization in skin wound healing in vivo.

Materials and Methods

Cell culture

Normal human epidermal keratinocytes (NHEK) were prepared and cultured under serum-free conditions, as previously described (Shirakata et al., 2000; Shirakata et al., 2003). Third- or fourth-passage cells were used in this study.

Table 1. Primer sequences for PCR

Wild-type HB-EGF – upper	5′-CATGATGCTCCAGTGAGTAGGCTCTGATTAC
Wild-type HB-EGF – lower	5′-AGGGCAAGATCATGTGTCCTGCCTCAAGCC
lox HB-EGF – upper	5′-ATGGGATCGGCCATTGAACA
lox HB-EGF – lower	5′-GAAGAACTCGTCAAGAAGGC
cre-recombinase – upper	5′-TTACCGGTCGATGCAACGAGTGATG
cre-recombinase – lower	5′-TTCCATGAGTGAACGAACCTGGTCG
lox-out HB-EGF – upper	5′-CGGACAGTGCCTTAGTGGAACCTC
lox-out HB-EGF – lower	5′-GCTTCTTCTTAGGAGGGATCTTGGC

Table 2. Primer sequences for RT-PCR

hHB-EGF – upper	5′-CCACACCAAACAAGGAGGAG
hHB-EGF – lower	5′-ATGAGAAGCCCCACGATGAC
hEPR – upper	5′-TCGCCCGCTCCCATCGCCG
hEPR – lower	5′-GGTTCCACATATTATTTCTG
hTGF-α – upper	5′-GAGTGCAGACCCGCCCGTGGC
hTGF-α – lower	5′-CCAGGAGGTCCGCATGCTCAC
hAR – upper	5′-CCAAAACAAGACGGAAAGTGA
hAR – lower	5′-AGGATCACAGCAGACATAAAG
hGAPDH – upper	5′-ACCACAGTCCATGCCATCAC
hGAPDH – lower	5′-TCCACCACCCTGTTGCTGTA
mHB-EGF – upper	5′-GGAATTCTGGAGCGGCTTCGGAGAG
mHB-EGF – lower	5′-CAAGCTTTGCAAGAGGGAGTACGGAACT
mEPR – upper	5′-GGAATTCTGACGCTGCTTTGTCTAGGTT
mEPR – lower	5′-CAAGCTTTATGCATCCAGCGGTTATGAT
mTGF-α – upper	5′-GGAATTCCTAGCGCTGGGTATCCTGTTA
mTGF-α – lower	5′-CAAGCTTACCACCACCAGGGCAGTGATG
mAR – upper	5′-CAAGCTTACCACCACCAGGGCAGTGATG
mAR – lower	5′-CAAGCTTACCACCACCAGGGCAGTGATG

h, human; m, mouse; EPR, epiregulin; AR, amphiregulin.

Generation of HB-EGF knockout mice using a gene targeting Cre-loxP strategy and PCR

The targeting construct has been described previously (Iwamoto et al., 2003). Homozygous $HB^{lox/lox}$ mice were bred with K5 promoter-driven Cre-recombinase transgenic mice to generate K5-Cre-$HB^{lox/+}$ mice (Takeda et al., 2000). Subsequently, K5-Cre-$HB^{lox/+}$ mice were bred with $HB^{lox/lox}$ mice to generate $HB^{lox/lox}$: K5-Cre ($HB^{-/-}$) mice. The genotype of each mouse was confirmed by PCR. Primers are shown in Table 1.

RT-PCR analysis

Keratinocytes were cultured in MCDB153 complete medium on type I collagen-coated dishes until they reached confluency. Keratinocytes were treated by tip scraping and total RNA was harvested at several time points. mRNA expression of HB-EGF, TGF-α, AR, EPR and GAPDH was analyzed by RT-PCR. The absence of HB-EGF mRNA in keratinocytes from $HB^{-/-}$ mice was confirmed by RT-PCR. Primers are shown in Table 2. The RT-PCR was performed using RT-PCR High Plus (Toyobo Co. Ltd, Osaka, Japan) according to the manufacturer's instructions. cDNA was reverse-transcribed from total RNA for 30 minutes at 60°C and heated to 94°C for 2 minutes. Amplification was performed using a DNA thermal cycler (Astec, Fukuoka, Japan) for 25 cycles. A cycle profile consisted of 1 minute at 94°C for denaturation, 1.5 minutes at 60°C for annealing and primer extension.

Wound healing studies

Wound healing experiments were performed in $HB^{-/-}$ and $HB^{lox/lox}$ mice. Under sodium pentobarbital anesthesia, two full-thickness wounds were created on the skin of the backs of each of nine 9- to 10-week-old female mice using 6-mm skin biopsy punches. Each wound diameter was determined as the average of longitudinal and lateral diameter. Wound closure was monitored, and skin sections were harvested at 3, 5, 7, 9 and 11 days after wounding. For BrdU labeling, mice received intraperitoneal injections of BrdU (250 μg/g; Sigma, Tokyo, Japan) 2 hours prior to sacrifice.

Histological analysis

Mouse tissues were fixed in 4% paraformaldehyde or formaldehyde, dehydrated and embedded in paraffin. Four-μm sections were stained with Hematoxylin and Eosin. For β-gal staining, after fixation with 0.2% glutaraldehyde and 1% formalin, the tissues were stained with 5-bromo-4-chloro-3-indol β-D-galactoside (X-gal). Skin sections were stained with rabbit anti-keratin IgG or anti-BrdU IgG, and immunopositive reactions were visualized using a streptavidin-biotin-peroxidase staining kit (Nichirei Co. Inc., Tokyo, Japan) according to the manufacturer's instructions. Morphometric analysis was performed using MacSCOPE Ver2.61 software. Statistical analysis was performed using Student's *t*-test.

Results

HB-EGF mRNA induction after in vitro scrape wound

To investigate the distinct role of HB-EGF in skin wound healing of the growth factors produced by NHEK, we first examined the induction of EGFR-ligand mRNA in NHEK in an in vitro wound-healing model. Confluent cultures of NHEK were scraped with a yellow pipette tip; total RNA was harvested at several time points, and the expression of growth-factor mRNAs was analyzed by RT-PCR. HB-EGF mRNA was rapidly induced after scraping, reaching a peak of 2.6-fold induction at 1 hour, whereas AR, TGF-α and EPR mRNAs were only slightly induced, with a maximum 1.5-fold increase (Fig. 1A). This indicates that HB-EGF is the most inducible gene of the EGFR ligands in NHEK. In normal mouse keratinocytes, HB-EGF was again the EGF family member that was induced predominantly after scraping, with a maximum 4.0-fold increase at 2 hours (Fig. 1B). EPR was also induced to a lesser degree, with a maximum 2.5-fold induction. TGF-α and AR were not induced after scraping. These results indicated that HB-EGF may play an important role in skin wound healing, and led us to investigate the in vivo function of HB-EGF.

Generation of keratinocyte-specific HB-EGF-deficient mice

Since germline targeting of the HB-EGF gene resulted in severe lethality (Iwamoto et al., 2003), we generated keratinocyte-specific HB-EGF-deficient mice ($HB^{lox/lox}$: K5-Cre, which we refer to as $HB^{-/-}$) using Cre/loxP technology in combination with the keratin 5 promoter (Takeda et al., 2000). $HB^{-/-}$ mice were identified by PCR analysis (Fig. 2A-C). The keratinocyte-specific absence of HB-EGF mRNA in $HB^{-/-}$

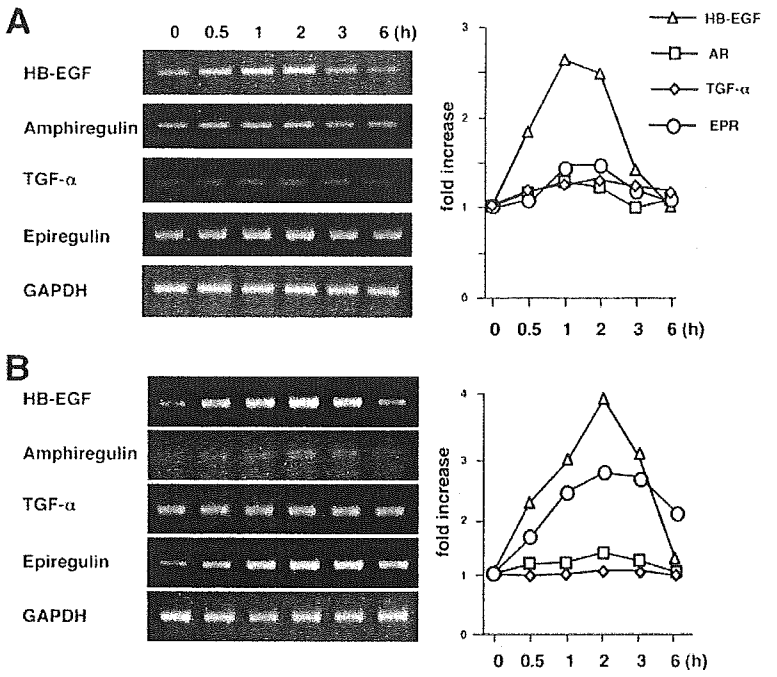

Fig. 1. Induction of expression of EGFR ligand mRNA, by scraping, in human and mouse keratinocytes. Confluent NHEK (A) and normal mouse epidermal keratinocytes (B) were scraped with a pipette tip; total RNA was harvested at several time points and mRNA expression was analyzed by RT-PCR. Right panels show densitometric analysis. In both cell types HB-EGF mRNA was rapidly and dramatically induced after scraping, whereas TGF-α, AR, and EPR mRNA were slightly induced in NHEK and the normal keratinocytes, although in the latter cells EPR was also increased.

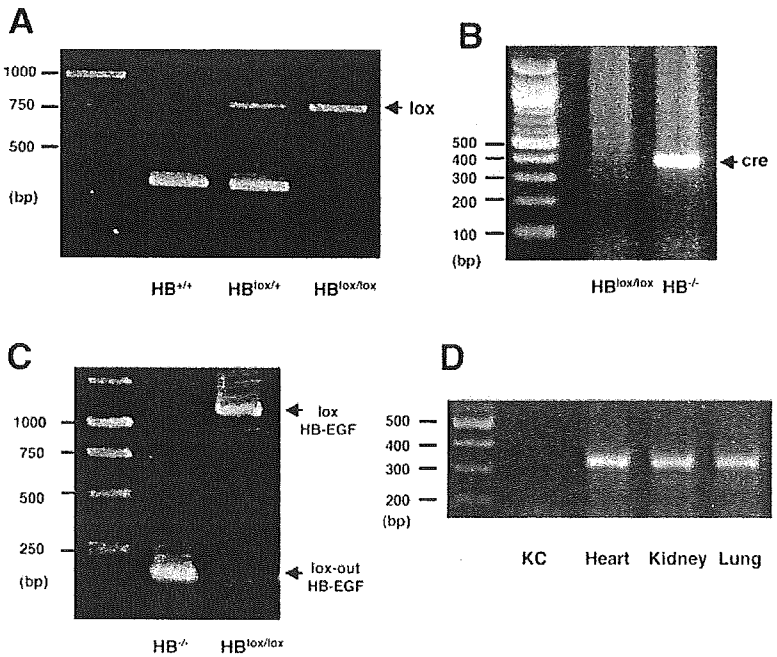

Fig. 2. Genotype of the keratinocyte-specific HB-EGF-deficient mice. (A-C) Keratinocyte-specific HB-EGF-deficient mice were confirmed by PCR as lox homozygous (A), Cre-recombinase positive (B) and lox-out (C). (D) Keratinocyte-specific disruption of HB-EGF mRNA in $HB^{-/-}$ mice was confirmed by RT-PCR. KC, keratinocytes.

mice was confirmed by RT-PCR (Fig. 2D). No apparent abnormalities were observed in the $HB^{-/-}$ mice.

Impaired wound healing in keratinocyte-specific HB-EGF-deficient mice

To examine the role of HB-EGF in skin wound healing in vivo, we performed a wound-healing assay using $HB^{lox/lox}$ and $HB^{-/-}$ mice. Two 6-mm punch skin biopsies were made in the back of each mouse and the wound diameter was measured at various times after wounding as a measure of healing. There was no difference in wound diameter up to day 3 post-wounding; however, wound healing was noticeably retarded from day 5 to 11 in the $HB^{-/-}$ mice. Wound closure was delayed significantly in $HB^{-/-}$ mice compared with $HB^{lox/lox}$ mice on day 8 (Fig. 3A). The wound diameter was reduced to 34% in $HB^{lox/lox}$ mice on day 8, whereas it was still 58% in the $HB^{-/-}$ mice (Fig. 3B). These results indicate that HB-EGF expression by keratinocytes is important for skin wound healing in vivo.

Cell proliferation was not impaired at the wound site in HB-/- mice

Since EGFR ligands promote NHEK proliferation and migration (Hashimoto, 2000), we investigated whether proliferation or migration was predominantly impaired in $HB^{-/-}$ mice. We measured the cell numbers in the leading edge of the biopsy wound and in the peripheral skin (1.2 mm from the wound margin) in $HB^{lox/lox}$ and $HB^{-/-}$ mice (Fig. 4A). After 48 hours, the total cells numbers were 90±13 and 65±19 in $HB^{lox/lox}$ and $HB^{-/-}$ mice, respectively, and after 72 hours 170±20 and 140±41 in $HB^{lox/lox}$ and $HB^{-/-}$, respectively (Fig. 4B). Since these small observed differences in cell numbers were not statistically significant, we investigated keratinocyte proliferation in $HB^{lox/lox}$ and $HB^{-/-}$ mice using a BrdU incorporation assay. Two hours before sacrifice, the mice received intraperitoneal injections of BrdU (250 μg/g). Skin samples were harvested, sectioned and stained with anti-BrdU antibody. Three days after wounding, there were no differences in the number or distribution of BrdU-positive cells between the $HB^{lox/lox}$ and $HB^{-/-}$ mice (Fig. 4C). These results suggest that delayed wound healing in $HB^{-/-}$ mice is not due to impaired cell proliferation in the epidermis.

Cell migration was impaired at the wound site in $HB^{-/-}$ mice

Since no impairment of proliferation was found, we next investigated whether migration was impaired in $HB^{-/-}$ mice. To quantify the migration

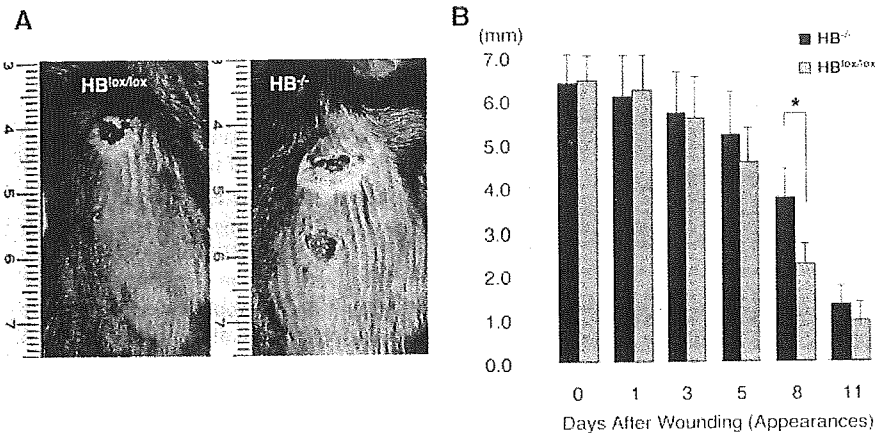

Fig. 3. Impaired wound healing in $HB^{-/-}$ mice. Two 6-mm punch biopsies were made in the skin of the backs of $HB^{lox/lox}$ and $HB^{-/-}$ mice, and wound diameter was monitored. (A) Macroscopic view of wound healing assay in $HB^{lox/lox}$ and $HB^{-/-}$ mice at day 8. (B) Measurements of wound diameter during healing. *$P<0.05$.

of keratinocytes in wound healing, we measured the length of the leading edge in each wound of $HB^{lox/lox}$ and $HB^{-/-}$ mice in the wound-healing assay. Sections of skin from the wound area were stained with anti-keratin IgG (Fig. 5A). On day 7 post-wounding, the epidermis had migrated toward the center of the wound in $HB^{lox/lox}$ mice, whereas keratinocytes remained near the wound margin and the epidermis had not spread in $HB^{-/-}$ mice, suggesting that keratinocyte migration was impaired in $HB^{-/-}$ mice (Fig. 5B). We then prepared skin sections from all the samples from the wound-healing assay and calculated the ratio of leading edge to initial wound length, using computer-assisted morphometric analysis. On day 3 post-wounding, there was no difference in the leading edge ratio between $HB^{lox/lox}$ and $HB^{-/-}$ mice. However, the leading edge ratio was decreased markedly in $HB^{-/-}$ mice after day 3. The ratio was 30.7% in $HB^{-/-}$ and 44.5% in $HB^{lox/lox}$ on day 5, and 38% in $HB^{-/-}$ and 65% in $HB^{lox/lox}$ mice on day 7 (Fig. 5C). The difference on day 7 was statistically significant. These results suggest that endogenous HB-EGF is an important growth factor for the migration of epidermis in skin wound healing.

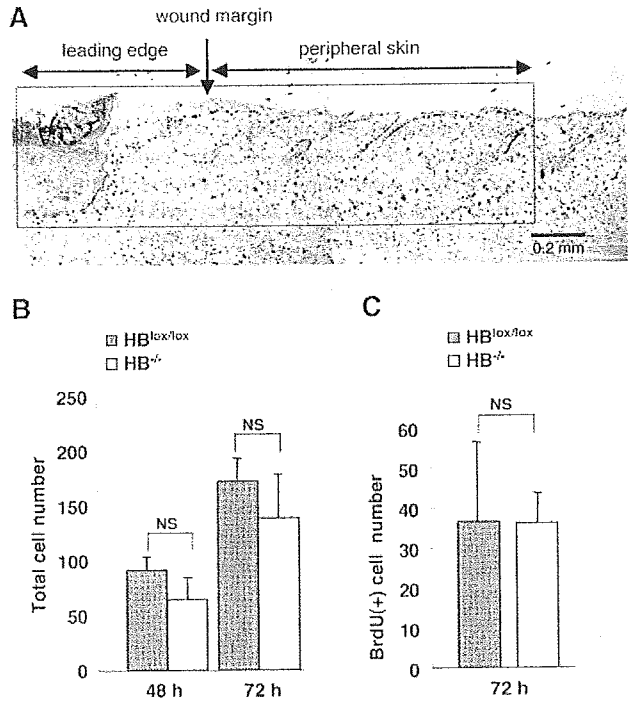

Fig. 4. BrdU-positive cell distribution at the leading edge and in the peripheral skin in $HB^{lox/lox}$ and $HB^{-/-}$ mice. (A) Skin sections were stained using anti-BrdU antibody, and cell numbers in the leading edge and in the peripheral skin were counted as indicated. (B) The total cell numbers in the peripheral skin (1.2 mm from the wound margin) and in the leading edge. (C) BrdU-positive cell number in the peripheral skin and in the leading edge. There were no differences in BrdU-positive cell numbers between $HB^{lox/lox}$ and $HB^{-/-}$ mice.

Expression of HB-EGF at wound sites

It has been reported that HB-EGF was upregulated in burn wound healing and that topical application of HB-EGF accelerated re-epithelialization of partial-thickness burns (Cribbs et al., 2002; Cribbs et al., 1998; McCarthy et al., 1996). It has been also reported that addition of HB-EGF into c-jun null keratinocyte growth medium can rescue the migration defect and induce phosphorylation of EGF receptor (Li et al., 2003). Since HB-EGF may play an important role in skin wound healing, we investigated the HB-EGF expression and keratinocyte proliferation pattern in skin wound healing using $HB^{lox/+}$:K5-Cre ($HB^{+/-}$) mice. With the targeting vector containing the *lacZ* gene as a reporter for the expression of HB-EGF, it is possible to ascertain the expression of HB-EGF by staining for β-gal in $HB^{+/-}$ mice. HB-EGF was expressed at the leading edge of the epithelium at day 2 post-wounding, and was predominantly expressed at the tip of the leading edge until day 7 (Fig. 6A). Unlike the HB-EGF expression pattern, BrdU-positive (BrdU+) cells were detected mainly within the peripheral skin on days 2 and 3. On days 5 and 7, BrdU+ cells were found toward the leading edge, although they were preferentially located near the wound margin. To quantify the distribution of HB-EGF-expressing cells and proliferating cells, we counted the β-gal-positive (β-gal+) cells and BrdU+ cells in 0.2 mm ranges in the leading edge and in the peripheral skin in $HB^{+/-}$ mice. On day 2 the peak of the β-gal+ cells was between 0 +0.2 mm into the leading edge, whereas the peak of the BrdU+ cells was –0.2 to –0.4 mm into the peripheral skin. On day 3, the peak of the β-gal+ cells was between +0.4 and +0.6 mm, whereas the peak of the BrdU+ cells was between 0